



UNIVERSITI
TEKNOLOGI
PETRONAS

**Modelling Inflow Performance of Multilateral Wells by Integration of Numerical and
Analytical Approach**

by

Siti Mariam Annuar

Dissertation submitted in partial fulfilment of
the requirement for the
MSc. Petroleum Engineering

18th July 2012

Universiti Teknologi PETRONAS
Bandar Seri Iskandar
31750 Tronoh
Perak Darul Ridzuan

CERTIFICATE OF APPROVAL

Modelling Inflow Performance of Multilateral Wells by Integration of Numerical and
Analytical Approach

by

Siti Mariam Annuar

Dissertation submitted in partial fulfilment of
the requirement for the
MSc. Petroleum Engineering

18th JULY 2012

Approved by,

AP Dr. Ismail M Saaid
Mr. Mohammad Amin Shoustari

UNIVERSITI TEKNOLOGI PETRONAS

TRONOH, PERAK

18th July 2012

CERTIFICATION OF ORIGINALITY

This is to certify that we are responsible for the work submitted in this project, that the original work is my own except as specified in the reference and acknowledgements, and that the original work contained herein have not been undertaken or done by unspecified sources or persons.

SITI MARIAM ANNUAR

ABSTRACT

Multilateral wells have emerged as a new means, alternative to vertical and horizontal wells for optimal reservoir exploitation. The single wellbore requires fewer production well slots hence reduces cost of rig time, tools, services and equipment together with increased and accelerated reserves. The main objective of this project is to develop a swift novel approach to predict and assess inflow performance of multilateral wells. Two modelling techniques are applied that is by using numerical and analytical approach. Numerical approach implements production optimization software tools to model the multilateral well inflow performance and perform sensitivity analysis against varying reservoir condition. Analytical approach employs horizontal inflow performance models to determine the multilateral well deliverability and perform sensitivity analysis against different well configuration. The single phase inflow performance models considered in this project are Joshi's model (1988), Butler model (1994) Furui *et al.*, model (2003), Babu and Odeh model (1989) and Helmy and Wattenbarger model (1998). The analysis is done under two different conditions: Steady-state and pseudo-steady state condition, for dual-lateral and tri-lateral well. Hypothetical reservoir and well data is used to generate similar inflow performance models for numerical and analytical approach. The models from two different approaches are compared and the analytical model that give the least percentage of difference from PROSPER model is selected to perform the sensitivity study. The inflow performance models simulated by both approaches show a combination of straight line and Vogel inflow performance model. For dual-lateral and tri-lateral well under steady-state condition the analytical model that gives the closest match to PROSPER model is Butler model (1994). For dual-lateral and tri-lateral well under pseudo-steady state condition the model that gives the least percentage of difference with PROSPER model is Helmy and Wattenbarger model (1998) and Babu and Odeh model (1989) respectively. The significance of this study is because prediction of well performance is one of the key factors in deciding the economic viability of a project. Estimates of well performance assist petroleum engineers to decide the optimum production and reservoir management plan.

ACKNOWLEDGEMENTS

My first gratitude would go to Allah SWT, all praise is due to Allah, and this project would not have been possible without His help. My sincere gratitude is extended to my supervisor Dr Ismail B. Mohd Saaïd and to my co-supervisor Mr. Mohammad Amin Shoustari, I am grateful to their commitment and encouragement throughout the project. I would like to thank Dr. Ding Zhu for her valuable advice and her generosity. I would also like to thank my colleagues, Chua Ai Tieng and Lydia Yusof for their friendship and help during my project. Finally, my gratitude goes to my family for their devotion and love.

TABLE OF CONTENTS

CHAPTER 1.....	1
1.1 BACKGROUND OF STUDY	1
1.2 PROBLEM STATEMENT	4
1.3 OBJECTIVES OF STUDY	5
1.4 SCOPE OF STUDY	5
CHAPTER 2.....	6
2.1 NUMERICAL APPROACH.....	6
2.1.1 Infinite conductivity	6
2.1.2 Finite conductivity	7
2.2 ANALYTICAL APPROACH.....	7
2.2.1 Steady-state condition	7
2.2.2 Pseudo-steady state condition	13
2.3 COMPARE AND CONTRAST ON ANALYTICAL MODELS.....	16
2.4 RESERVOIR INFLOW PERFORMANCE.....	17
2.4.1 Liquid Inflow	17
2.4.2 Gas Inflow	18
2.4.3 Two phase (Gas-Liquid) Inflow	19
CHAPTER 3.....	21
3.1 DUAL-LATERAL WELL.....	21
3.1.1 Steady-state condition	21
3.1.2 Pseudo-steady state condition	23
3.2 TRI-LATERAL WELL.....	24
3.2.1 Steady-state condition	24
3.2.2 Pseudo-steady state condition	26
3.3 MODELLING PROCEDURES.....	26
3.4 WORKFLOW SUMMARY	28
CHAPTER 4.....	29
4.1 STEADY-STATE CONDITION	29
4.1.1 Reservoir Inflow Performance	29
4.1.2 Comparison and Matching Process.....	35

4.2	PSEUDO- STEADY STATE CONDITION	39
4.2.1	Reservoir Inflow Performance	39
4.2.2	Comparison and Matching Process.....	43
4.3	SENSITIVITY STUDY	47
CHAPTER 5		53
APPENDICES		57
Appendix A		57
Appendix B		58
Appendix C		60

LIST OF FIGURES

Figure 1.1: A schematic diagram of a multilateral well [3]	1
Figure 1.2: Typical multilateral wells for petroleum productions [10]	3
Figure 2.1: The geometry assumed for Joshi's Model (1988) [13]	8
Figure 2.2: Flow geometry in a box-shaped reservoir [13]	10
Figure 2.3: The system schematic of Babu and Odeh's model [13]	13
Figure 2.4: Straightline IPR (for an incompressible liquid) [16]	17
Figure 2.5: Gas well deliverability reduced by non-Darcy flow pressure losses [16].	19
Figure 2.6: Inflow Performance Relationships [16]	20
Figure 3.1: A schematic diagram of a dual-opposed lateral well	22
Figure 3.2: A schematic diagram of a tri-lateral well	25
Figure 3.3: Workflow of the modelling procedure	27
Figure 3.4: Workflow summary	28
Figure 4.1: IPR from PROSPER under infinite conductivity for dual-lateral well	30
Figure 4.2: IPR from PROSPER under infinite conductivity for tri-lateral well	31
Figure 4.3: IPR of the steady-state analytical models for dual-lateral well	32
Figure 4.4: IPR steady-state analytical models for tri-lateral well	33
Figure 4.5: IPR of PROSPER and steady-state analytical models for dual-lateral well	35
Figure 4.6: IPR of PROSPER and steady-state analytical models for tri-lateral well.	37
Figure 4.7: IPR from PROSPER under finite conductivity for dual-lateral well	39
Figure 4.8: IPR from PROSPER under finite conductivity for tri-lateral well	40
Figure 4.9: IPR of the pseudo-steady state analytical models for dual-lateral well	41
Figure 4.10: IPR of the pseudo-steady state analytical models for tri-lateral well	42
Figure 4.11: IPR of PROSPER and pseudo-steady state analytical models for dual- lateral well	43
Figure 4.12: IPR of PROSPER and pseudo-steady state analytical models for tri- lateral well	45
Figure 4.13: Effect of lateral lengths on the IPR under steady-state condition	47
Figure 4.14: Effect of lateral lengths on the IPR under pseudo-steady condition	48
Figure 4.15: Effect of GOR on the IPR under steady-state condition	49
Figure 4.16: Effect of GOR on the IPR under pseudo-steady state condition	49

Figure 4.17: Effects of oil gravity on the IPR under steady-state condition.....	51
Figure 4.18: Effects of oil gravity on the IPR under pseudo-state condition	51
Figure A.1: TAML classification for multilateral wells [18]	57

LIST OF TABLES

Table 2.1: Summary of the similarities and differences of the analytical models used in this research project	16
Table 3.1: Reservoir and well data for a dual-lateral well [8]	21
Table 3.2: PVT data for dual-lateral well	22
Table 3.3: Reservoir and well data for a tri-lateral well [17].....	24
Table 3.4: PVT data for tri-lateral well.....	25
Table 4.1: Comparison of the AOF of PROSPER and steady-state analytical models	36
Table 4.2: Comparison of the percentage difference between the IPR of PROSPER and steady-state analytical models for dual-lateral well	36
Table 4.3: Comparison of the AOF of PROSPER and steady-state analytical models	38
Table 4.4: Comparison of the percentage difference between the IPR of PROSPER and steady-state analytical models for tri-lateral well	38
Table 4.5: Comparison of the AOF of PROSPER and pseudo-steady state analytical models for dual-lateral well	44
Table 4.6: Comparison of the percentage difference between the IPR of PROSPER and pseudo-steady state analytical models for dual-lateral well.....	44
Table 4.7: Comparison of the AOF of PROSPER and pseudo-steady state analytical models for tri-lateral well.....	46
Table 4.8: Comparison of the percentage difference between the IPR of PROSPER and pseudo-steady state analytical models for tri-lateral well	46

ABBREVIATIONS

TAML	Technical Advancement Multilaterals
PROSPER	Production System Performance
PETEX	Petroleum Experts
IPR	Inflow Performance Relationship
GOR	Gas Oil Ratio
AOF	Absolute Open Flow
PVT	Pressure Volume Temperature
FEM	Finite Element Model
PI	Productivity Index
B&O	Babu and Odeh model (1989)
H&W	Helmy and Wattenbarger model (1998)

NOMENCLATURES

Symbol	Description	Units
q	Flowrate	STB/day
k_H	Horizontal permeability	md
k_V	Vertical permeability	md
I_{ani}	Anistropy ratio	Dimensionless
k_y	Permeability of formation in y-direction	md
k_x	Permeability of formation in x-direction	md
k_z	Permeability of formation in z-direction	md
\bar{P}	Average reservoir pressure	Psia
P_e	Pressure at the external radius ($r = r_e$)	Psia
P_{wf}	Bottomhole flowing pressure	Psia
μ	Viscosity	psi ⁻¹
B_o	Formation Volume Factor	res bbl/STB
T	Temperature of reservoir	°F
r_w	Wellbore radius	ft
r_{eH}	Equivalent cylinder drainage radius	ft
$\ln C_H$	Shape factor	Dimensionless
s	Skin due to formation damage	Dimensionless
S_R	Partial penetration skin	Dimensionless
P_{xyz}	Partial penetration skin component x-y-z plane	Dimensionless
P'_{xy}	Partial penetration skin component x-y plane	Dimensionless
P_y	Partial penetration skin component y-plane	Dimensionless
a	Width of reservoir	ft
b	Length of reservoir	ft
h	Height of the reservoir	ft
L	Length of lateral	ft
A	Drainage area	ft ²
x_0	Well location in x-direction	ft
y_0	Well location in y-direction	ft

z_0	Well location in z-direction	ft
x_{mid}	x-coordinate of the midpoint of the well	ft

CHAPTER 1

INTRODUCTION

1.1 BACKGROUND OF STUDY

Prediction of well performance is one of the key factors in deciding the economic viability of a project. Estimates of well performance are very important to Petroleum engineer to decide the optimum production plan as well as reservoir management plan [1]. This project focuses on inflow performance of multilateral wells. The definition of multilateral well is a well which has more than one lateral or branch, either inclined or horizontal, connected to a single or mother wellbore [2]. Figure 1.1 below shows a basic schematic diagram of a multilateral well configuration [3].

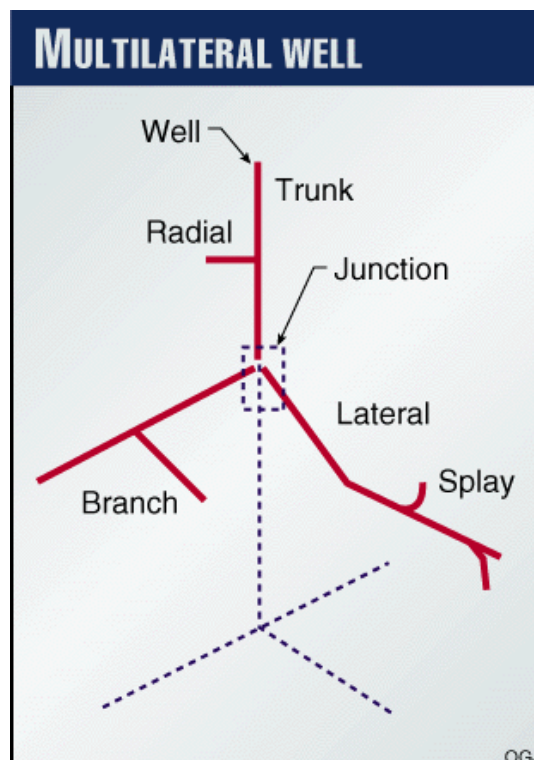


Figure 1.1: A schematic diagram of a multilateral well [3]

Multilateral wells have emerged as a new means, alternative to vertical and horizontal wells, for optimal reservoir exploitation. Significant advances in drilling and completion technologies encourage the development of this unconventional well [4]. The wells have various level of sophistication in their design which ranges from level 1 to level 6, where level 1 being the simplest openhole sidetracks to level 6 where the branches could be re-entered or isolated selectively [5].

Described below are the technical and economical benefits of multilateral wells:

- a) **Minimization of wellbore pressure losses:** A multilateral well is a better alternative to a long single lateral because as the well length increases the transportation of large volumes of fluid result in considerable pressure loss consequently decreasing well productivity [6]. Stated in the SPE book by Hill *et al.*, 2008 “Two opposing laterals, each of a certain moderate length would produce in many cases at least 50% larger production rate than a single horizontal well as long as or longer than the sum of the lengths of the two opposing laterals” [7].
- b) **Increased reserves:** The geometry of multilateral wells enabled better reservoir coverage. For example from Figure 1.5 (b) shows a four stacked multilateral wells, this well configuration improves drainage and sweep efficiency for heavy oil reserves in thick formation [8] and also Figure 1.5 (d), the herringbone multilateral well structure intersects more than one isolated pockets of reservoir increasing the reserves.
- c) **Cost reduction and slot conservation:** The single wellbore requires fewer production well slots hence reduces cost of rig time, tools, services and equipment. The total cost of a multilateral well could be higher than the cost of a vertical or horizontal completion [8]. However, the benefit can possibly overcome the cost; this has been proven by the first multilateral well drilled in Russia, the cost is 1.5 times more than conventional wells however production increases by 17 times more oil per day [9].

Figure 2 below show examples of geological settings and the appropriate multilateral well architecture to develop the reservoir:

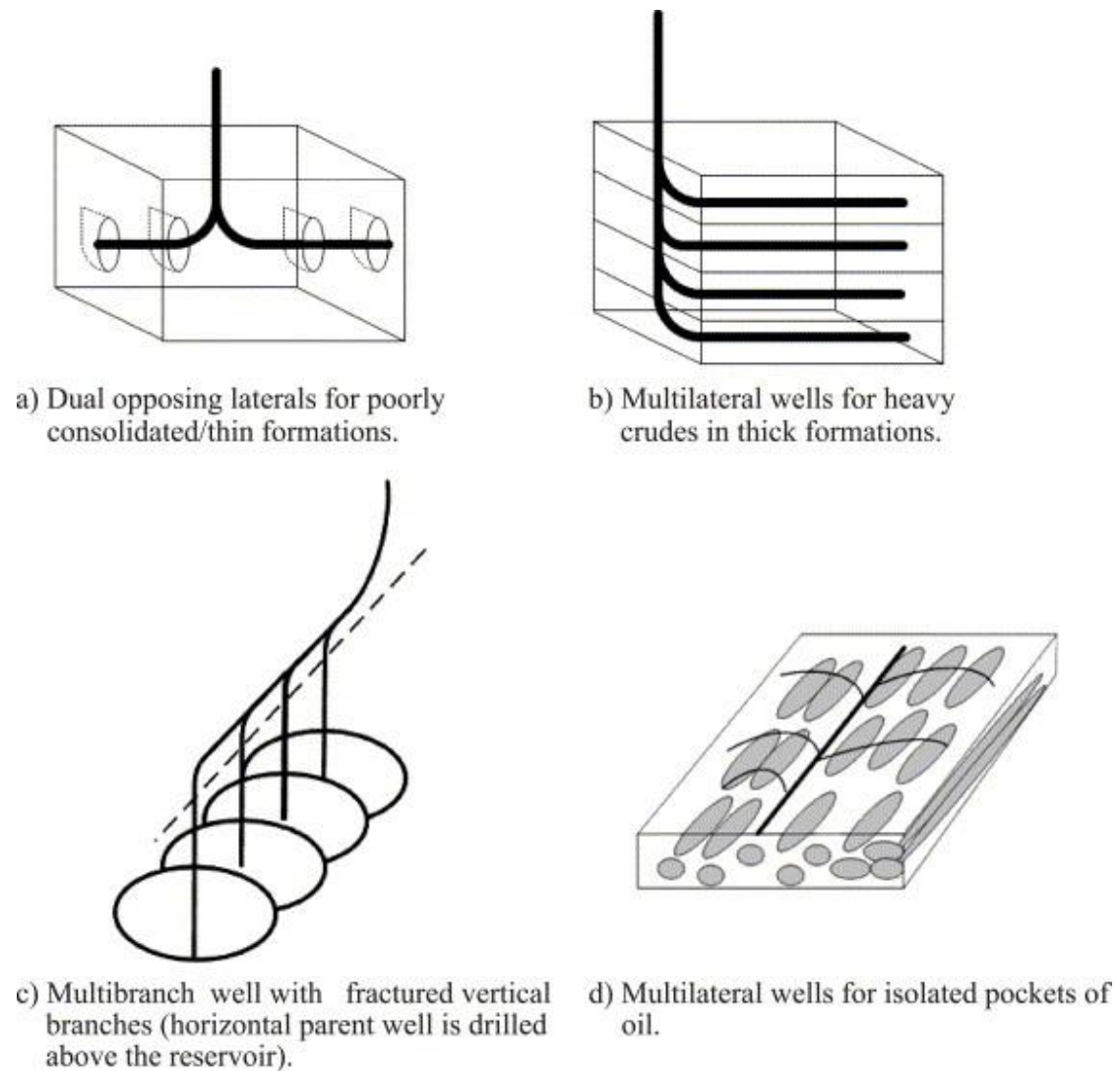


Figure 1.2: Typical multilateral wells for petroleum productions [10]

1.2 PROBLEM STATEMENT

The common issue in oil production is as the well ages, reservoir pressure depletes together with an increase in water cut which may cause the well to cease production altogether. Furthermore, modelling multilateral wells is complex for particular configurations and geological structure hence to overcome these problems engineers must be able to predict multilateral well performance [11]. It is very crucial to develop a reliable and accurate method to determine multilateral well performance for optimum production scheme, design production and artificial lift equipment, design simulation treatments and forecast production for planning purposes. Each of these items is an integral part of the efficient operation of producing wells and successful reservoir management [1].

The modelling techniques applied to assess and optimize well performance are by using a production optimization software tool from Petroleum Experts (PETEX) known as PROSPER (Production System Performance). The main purpose of the software is to model the inflow performance of multilateral wells and perform sensitivity studies of well design against varying reservoir condition. Another technique is by applying analytical models to determine the inflow performance and perform sensitivity study of well design against different well configurations. Sensitivity analysis provides estimation of the well productivity under today's actual or future producing conditions [2]. Therefore to proceed with the present investigation analytical models are applied to perform sensitivity on the lateral length and PROSPER is implement to perform the sensitivity on the reservoir conditions.

1.3 OBJECTIVES OF STUDY

The main objective of this project is to develop a novel approach to predict and optimize inflow performance of multilateral wells. Two modelling techniques are applied that is by using numerical and analytical approach. The main objective can be further refined to the following list below:

- a) To determine inflow performance of multilateral wells through numerical and analytical approach by incorporating identical hypothetical reservoir and well data.
- b) To model sensitivity study on the inflow performance models against varying Gas Oil Ratio (GOR), oil gravity and lateral length.

1.4 SCOPE OF STUDY

Stated in the Production technology notes the most common multilateral well has two or three laterals per well. This is because they are often implemented in fields where horizontal wells were successful and to further save cost is by having fewer wellbores to surface. This project focuses on modelling inflow performance of a dual- lateral and tri-lateral wells for which the branches are horizontal or close to horizontal in the reservoir [2]. The analysis of the multilateral wells is done separately for a steady-state and pseudo-steady state conditions for single phase oil wells.

CHAPTER 2

LITERATURE REVIEW

The two modelling techniques that is numerical and analytical approach are elaborated in this section:

2.1 NUMERICAL APPROACH

Currently, it is a common practice for Petroleum industry to employ PROSPER, a production optimization tool to evaluate well performance. The main reason PROSPER is selected for this project is because of its capability of modelling the performance of multilateral wells. The main applications of this software to the project are:

- a) Determine inflow performance of a dual-lateral and tri-lateral wells under two different conditions: Infinite conductivity and Finite conductivity.
- b) Modelling sensitivity analysis of the IPR against Gas Oil Ratio (GOR) and oil gravity.

Modelling of inflow performance in PROSPER will be performed under two different conditions:

2.1.1 Infinite conductivity

This option does not consider pressure drops in the pipes, therefore this option can be used to obtain the reservoir deliverability neglecting the pressure drop in the wellbore, from the reservoir to the Tie-point [12].

Note: Tie-point is the node for which the IPR is solved and is located at the top of the system (in vertical depth and hierarchically). Hence, the tie-point can only be a start point [12].

2.1.2 Finite conductivity

This option will calculate and consider the pressure drop across the branches and casing and it will include the interference of the branches as they produce from the same reservoir or in a communicating reservoir [12].

2.2 ANALYTICAL APPROACH

The beginning point of any multilateral well performance model is the reservoir inflow to a single lateral. Hill *et al.*, 2008 utilized horizontal well inflow performance (IPR) models that predict flow rate into the well as a function of reservoir drawdown. The technique selected to calculate the horizontal well IPR models is with simple analytical approach [13]. The models are summarized in two groups following the assumption of the boundary condition [14]:

2.2.1 Steady-state condition

In reservoir engineering, steady-state flow can only occur if fluid is injected over the outer boundary at the same rate, q , as it is produced at the well. The pressure at the wellbore, $r = r_w$, is denoted as P_{wf} while at the external radius, $r = r_e$, is denoted by P_e [15]. The initial reservoir pressure is maintained constant with the presence of aquifer (natural water influx or gas-cap expansion) or through injection wells (water-flooding).

a) Joshi's model (1988)

Joshi's model (1988) assumed ellipsoidal-shaped reservoir. The model divided the three-dimensional flow problem into two-dimensional problems to obtain the horizontal performance model. The model was modified by Economides *et al.*, 1991 to include the effects of anisotropy and formation damage (through skin factor). Joshi's model is derived for a well that is centred in the drainage volume, both vertically and horizontally. Joshi presented modification to the model to account for eccentricity in the vertical plane [13].

The diagram below presents the ellipsoidal-shaped reservoir assumed by Joshi:

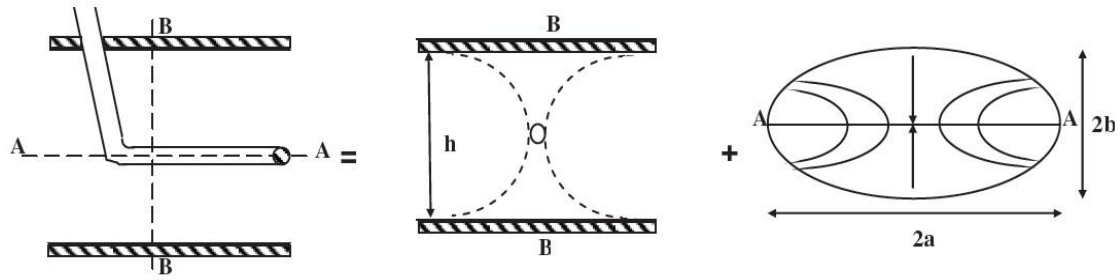


Figure 2.1: The geometry assumed for Joshi's Model (1988) [13]

Joshi's model (1988) is presented below:

$$q = \frac{k_H h (P_e - P_{wf})}{141.2 \mu B_o \left[\ln \left(\frac{a + \sqrt{a^2 - \left(\frac{L}{2}\right)^2}}{\frac{L}{2}} \right) + \frac{I_{ani} h}{L} \left(\ln \left(\frac{I_{ani} h}{r_w (I_{ani} + 1)} \right) + s \right) \right]} \quad - \quad (2.1)$$

Where the anisotropy ratio, I_{ani} , is defined as:

$$I_{ani} = \sqrt{\frac{k_H}{k_V}} \quad - \quad (2.2)$$

Drainage area is evaluated as follows:

$$a = \frac{L}{2} \left\{ 0.5 + \left[0.25 + \left(\frac{r_{eH}}{\frac{L}{2}} \right)^4 \right]^{0.5} \right\}^{0.5} \quad - \quad (2.3)$$

Where,

q	=	Flowrate
k_H	=	Horizontal permeability
k_V	=	Vertical permeability
h	=	Height of the reservoir
P_e	=	Pressure at the external radius ($r = r_e$)
P_{wf}	=	Bottomhole flowing pressure
μ	=	Viscosity
B_o	=	Formation Volume Factor
a	=	Half length of the drainage ellipse
L	=	Length of lateral
I_{ani}	=	Anisotropy ratio
r_w	=	Wellbore radius
s	=	Skin due to formation damage
r_{eH}	=	Equivalent cylindrical drainage radius

There is a condition to use Joshi's model:

$$L > h \text{ and } \left(\frac{L}{2}\right) < 0.9 r_{eH}$$

b) Butler model (1994)

Butler model (1994) assumed a horizontal well fully-penetrating a box-shaped reservoir, located midway between the upper and lower boundaries based on the image well superposition solution. The equation can evaluate both isotropic and anisotropic reservoir [14]. The figure below illustrates the flow geometry assumed by Butler model:

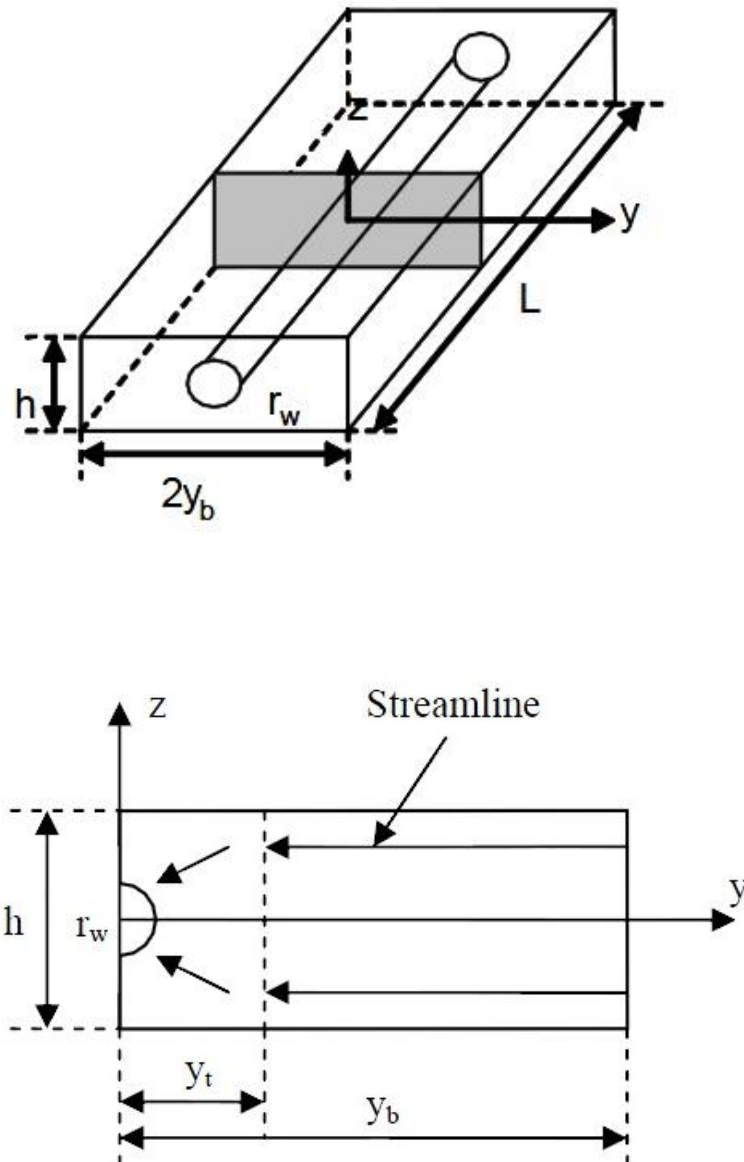


Figure 2.2: Flow geometry in a box-shaped reservoir [13]

Butler model (1994) is presented below:

$$q = \frac{k_H L (P_e - P_{wf})}{141.2 \mu B_o \left[I_{ani} \ln \left[\frac{I_{ani} h}{r_w (I_{ani} + 1) \sin \left(\frac{\pi y_b}{h} \right)} \right] + \frac{\pi y_b}{h} - 1.14 + s \right]} \quad - \quad (2.4)$$

Where,

- q = Flowrate
- k_H = Horizontal permeability
- k_V = Vertical permeability
- h = Height of reservoir
- P_e = Pressure at the external radius ($r = r_e$)
- P_{wf} = Bottomhole flowing pressure
- μ = Viscosity
- B_o = Formation Volume Factor
- L = Length of lateral
- I_{ani} = Anisotropy ratio
- r_w = Wellbore radius
- s = Skin due to formation damage
- y_b = Well location in y-direction

c) Furui *et al.*, model (2003)

Furui *et al.*, model (2003) presented an analytical model using the same assumption on the flow geometry as illustrated in Figure 2.2. The model assumes a horizontal well fully penetrates a box-shaped reservoir, located in the centre of the reservoir with no-flow boundaries at the top and bottom of the reservoir and constant pressure at the reservoir boundaries in the y-direction. The flow near the well is radial and becomes linear farther from the well. The model can also be used to evaluate both isotropic and anisotropic reservoir. A skin factor was added to the model to include the effect of

formation damage on well productivity. This model was based on the simulation results of a finite element model (FEM) for incompressible fluid [14].

Furui *et al.*, model (2003) is presented below:

$$q = \frac{kL(P_e - P_{wf})}{141.2\mu B_o \left[\ln \left(\frac{I_{ani} h}{r_w (I_{ani} + 1)} \right) + \frac{\pi y_b}{I_{ani} h} - 1.224 + s \right]} \quad - \quad (2.5)$$

Where k is defined as,

$$k = \sqrt{k_y k_z} \quad - \quad (2.6)$$

Where,

q	=	Flowrate
k_H	=	Horizontal permeability
k_V	=	Vertical permeability
h	=	Height of the reservoir
P_e	=	Pressure at the external radius ($r = r_e$)
P_{wf}	=	Bottomhole flowing pressure
μ	=	Viscosity
B_o	=	Formation Volume Factor
L	=	Length of lateral
I_{ani}	=	Anisotropy ratio
r_w	=	Wellbore radius
s	=	Skin due to formation damage
y_b	=	Well location in y-direction
k_y	=	Permeability of formation at y-direction
k_z	=	Permeability of formation at z-direction

2.2.2 Pseudo-steady state condition

In many reservoir situations there is no natural water influx or gas-cap expansion and in the absence of artificial fluid injection causes the reservoir pressure to decline in a uniform manner [15]. Average reservoir pressure is incorporated in the IPR equation, \bar{P} .

a) Babu and Odeh model (1989)

Assumption on the geometry model used by Babu and Odeh model (1989) is shown in Figure 2.3. The model uses shape factor to consider for drainage change and a partial penetration skin factor for partial penetrated wellbores. The model can be used to evaluate both isotropic and anisotropic reservoirs and the well can be in any positions in the reservoir.

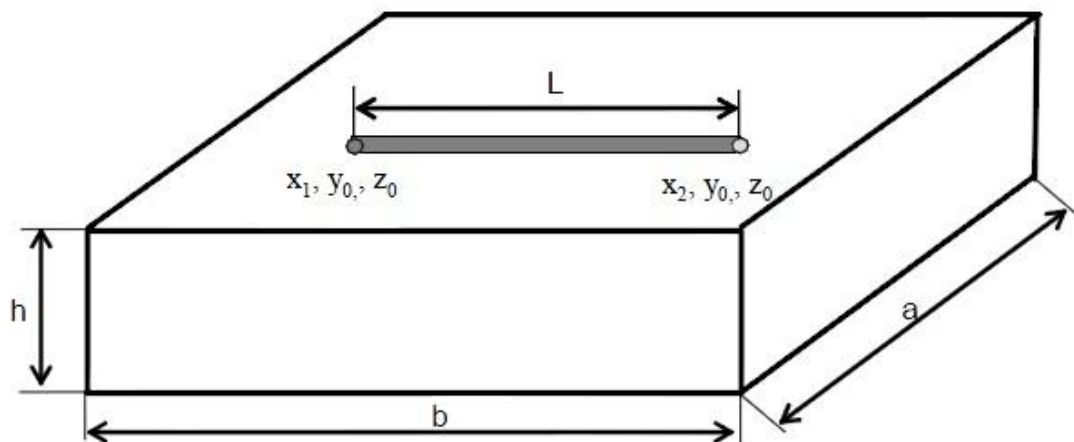


Figure 2.3: The system schematic of Babu and Odeh's model [13]

Babu and Odeh model (1989) is presented below:

$$q = \frac{\sqrt{k_y k_z} b (\bar{P} - P_{wf})}{141.2 \mu B_o \left[\ln \left(\frac{A^{0.5}}{r_w} \right) + \ln C_H - 0.75 + S_R + \left(\frac{b}{L} \right) s \right]} \quad - \quad (2.7)$$

Where $\ln C_H$ is defined as,

$$\ln C_H = 6.28 \frac{a}{I_{ani} h} \left[\frac{1}{3} - \frac{y_0}{a} + \left(\frac{y_0}{a} \right)^2 \right] - \ln \left(\sin \frac{\pi z_0}{a} \right) - 0.5 \ln \left[\frac{a}{I_{ani} h} \right] - 1.088 \quad - \quad (2.8)$$

Where,

q	=	Flowrate
k_H	=	Horizontal permeability
k_V	=	Vertical permeability
h	=	Height of the reservoir
\bar{P}	=	Average reservoir pressure
P_{wf}	=	Bottomhole flowing pressure
μ	=	Viscosity
B_o	=	Formation Volume Factor
L	=	Length of lateral
I_{ani}	=	Anistropy ratio
r_w	=	Wellbore radius
s	=	Skin due to formation damage
y_b	=	Well location in y-direction
k_y	=	Permeability of formation at y-direction
k_z	=	Permeability of formation at z-direction
$\ln C_H$	=	Shape factor
S_R	=	Partial penetration skin

b) Helmy and Wattenbarger model (1998)

Helmy and Wattenbarger model (1998) is an extended work of Babu and Odeh to the case of uniform wellbore pressure (as opposed to uniform flux along the well) by determining correlation constants for the Dietz shape factor and the partial penetration skin factor for this case. They also modified the partial penetration skin model of Babu and Odeh's for the uniform flux. The correlation was developed using correlation equations of Babu and Odeh, adding some additional empirical constants and then finding the constants in these equations that gave the best global match simulation results [13].

Helmy and Wattenbarger model (1998) is presented below:

$$J = \frac{k_{eq} b_{eq}}{141.2B\mu \left(\frac{1}{2} \ln \left(\frac{4A_{eq}}{\gamma r_{weq}^2} - \frac{1}{2} \ln C_A + S_R \right) \right)} \quad - \quad (2.9)$$

In the equations above, the subscript “eq” denotes the transformed variables used to describe an anisotropic reservoir and are defined in Appendix C.

2.3 COMPARE AND CONTRAST ON ANALYTICAL MODELS

Table 2.1: Summary of the similarities and differences of the analytical models used in this research project

	Boundary condition	Model geometry	Skin factor
Joshi's model (1988)	Steady-state	Ellipsoidal-shaped reservoir	Formation damage
Butler model (1994)	Steady-state	Box-shaped reservoir	Formation damage
Furui <i>et al.</i>, model (2003)	Steady-state	Box-shaped reservoir	Formation damage
Babu and Odeh model (1989)	Pseudo-steady state	Box-shaped reservoir	Formation damage and partial penetration skin
Helmy and Wattenbarger model (1998)	Pseudo-steady state	Box-shaped reservoir	Formation damage and partial penetration skin

Joshi's model (1988) is the only model that assumes different model geometry that is ellipsoidal-shaped reservoir. The model divided a three-dimensional flow problem into two dimensional problems to obtain the horizontal well performance. Butler model (1994) and Furui *et al.*, model (2003) are identical except for the constant 1.14 in the Butler model and 1.224 in the Furui *et al.*, model [13]. Therefore the expected results from Butler model and Furui *et al.*, model is to be similar. For Babu and Odeh model (1989) and Helmy and Wattenbarger model (1998) is also identical. Both models assume the same model geometry that is box-shaped reservoir and Helmy and Wattenbarger model (1998) is an extended work of Babu and Odeh model (1989). The steady-state analytical models are valid for fully penetrating horizontal well where the skin factor in the models is cause by formation damage. For pseudo-steady state analytical models are valid for fully penetrating and partially penetrating horizontal well where the skin factor in the models is cause by formation damage and fully or partially penetrated horizontal well.

2.4 RESERVOIR INFLOW PERFORMANCE

The Inflow Performance Relationship (IPR) is routinely measured using bottomhole pressure gauges at regular intervals as part of the field monitoring programme. This relationship between flowrate (q) and the wellbore pressure (P_{wf}) is one of the major building blocks for a nodal-type analysis of well performance [16].

2.4.1 Liquid Inflow

IPR for undersaturated oil:

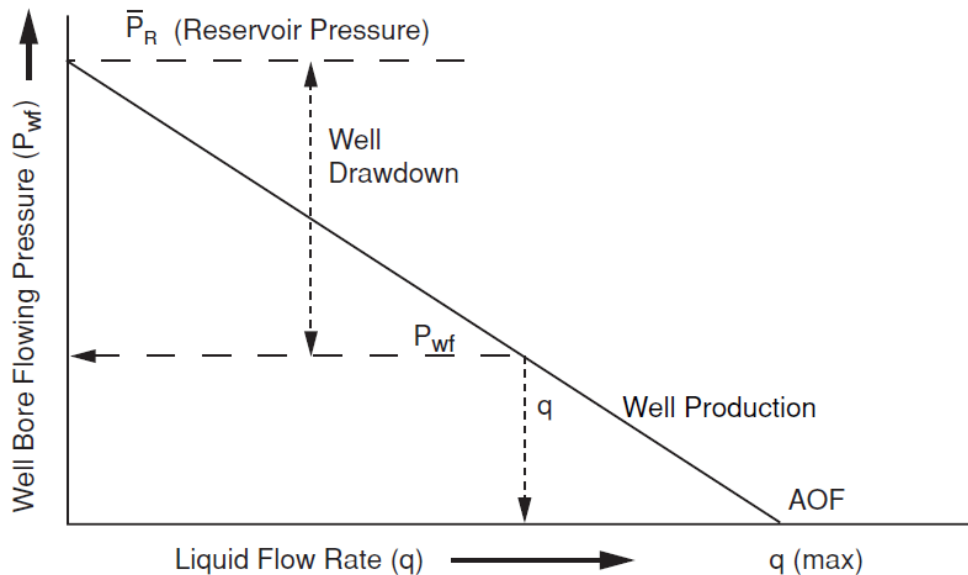


Figure 2.4: Straightline IPR (for an incompressible liquid) [16]

Straight line productivity equation is:

$$q = PI(\bar{P} - P_{wf}) \quad - \quad (2.10)$$

Where,

q	=	Flowrate	STB/day
PI	=	Productivity Index	STB/day/psi
\bar{P}	=	Average reservoir pressure	Psia
P_{wf}	=	Bottomhole flowing pressure	Psia

The Absolute Open Flow (AOF or q_{max}) is the flowrate when flowing bottomhole pressure is zero. AOF, although representing an unrealistic condition, is a useful parameter when comparing wells within a field since it combines PI and reservoir pressure in one number representative of well inflow potential [16].

2.4.2 Gas Inflow

The compressible nature of gas results in the IPR no longer being a straight line however the extension of this steady-state relationship from Darcy's Law, using an average value for the properties of the gas between the reservoir and wellbore leads to [16]:

$$q = C(\bar{P}_R^2 - P_{wf}^2) \quad - \quad (2.11)$$

Where C is a constant

Eq. 2.11 is valid for low flowrates, and becomes invalid at high flowrates because non-Darcy (or turbulent) flow effects begin to be observed. The equation for high flowrates is:

$$q = C(\bar{P}_R^2 - P_{wf}^2)^n \quad - \quad (2.12)$$

Where $0.5 < n < 1.0$

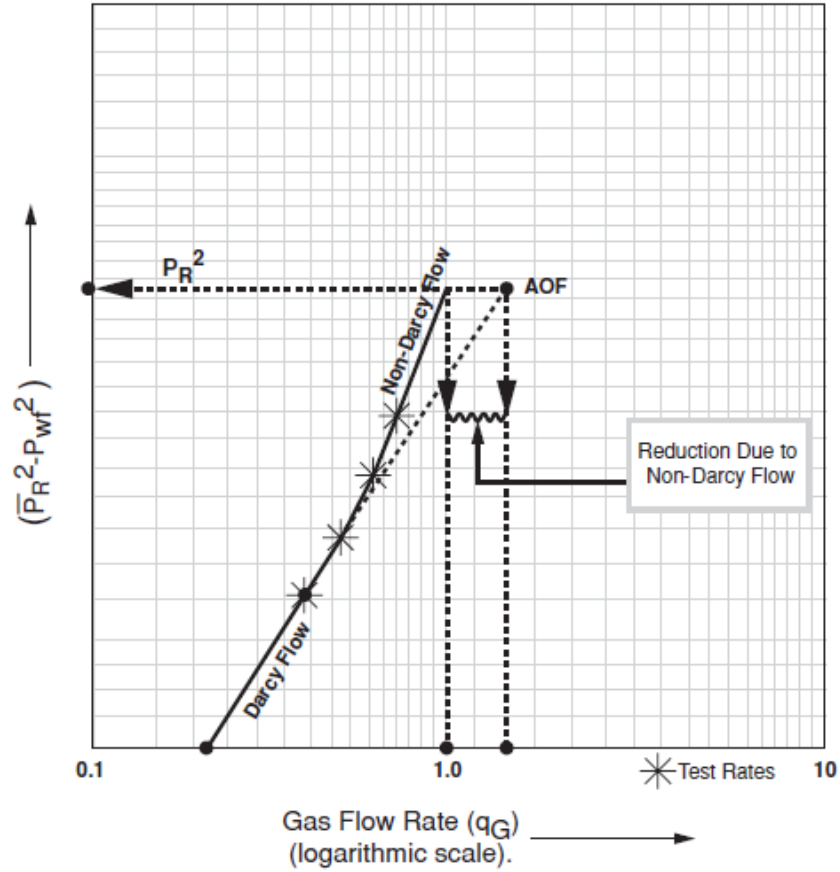


Figure 2.5: Gas well deliverability reduced by non-Darcy flow pressure losses
[16]

2.4.3 Two phase (Gas-Liquid) Inflow

Straight line IPR (Eq. 2.10) is not applicable when two phase inflow is occurring, e.g. when saturated oil is being produced. The equation for two-phase inflow is as follow:

$$\frac{q}{q_{max}} = 1 - 0.2 \left(\frac{P_{wf}}{\bar{P}} \right) - 0.8 \left(\frac{P_{wf}}{\bar{P}} \right)^2 \quad - \quad (2.13)$$

Figure 2.6 compares the production rate as a function of pressure drawdown for an undersaturated oil (straight line IPR, line A) and a saturated oil showing two phase flow effects discussed above (Curve B). Curve C is a case when the wellbore pressure is below the bubble point and the reservoir pressure is above the bubble point i.e. (incompressible) liquid flow is occurring in the bulk of the reservoir [16].

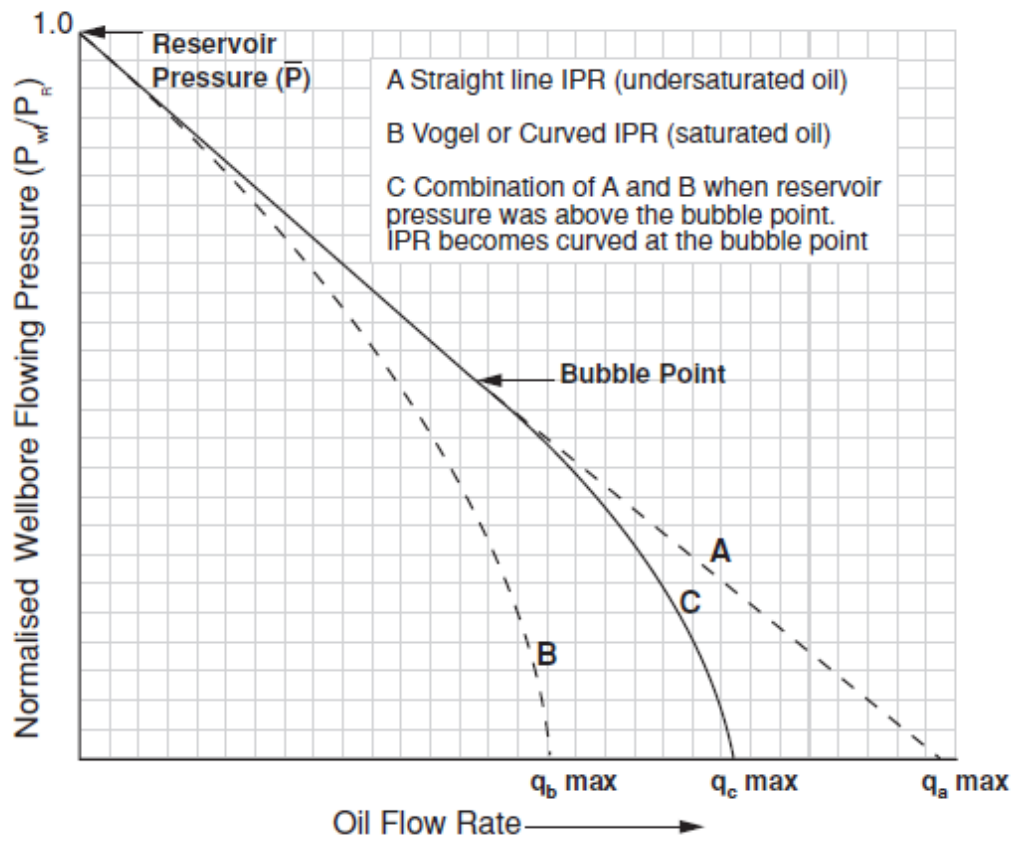


Figure 2.6: Inflow Performance Relationships [16]

In conclusion, it is important to study the analytical models and investigate which one of the model best represents IPR model simulated by PROSPER. The analytical model, which gives the closest match with IPR model from PROSPER, is selected to perform sensitivity study to well configuration. PROSPER focuses on sensitivity study against reservoir condition where as the analytical model focuses on sensitivity study against the well configuration.

CHAPTER 3

METHODOLOGY

This section elaborates on the modelling procedure of the inflow performance. The analysis is divided into two sections that is steady-state and pseudo-steady state condition.

3.1 DUAL-LATERAL WELL

3.1.1 Steady-state condition

a) Data availability

Table 3.1 presents an example of a hypothetical reservoir data for oil well taken from a dissertation by Dulce Maria Arcos Rueda, a thesis submitted to Texas A&M University in 2008. This data was used for the same purpose that is to assess multilateral well performance for a dual-lateral well.

Table 3.1: Reservoir and well data for a dual-lateral well [8]

Symbol	Description	Units	Pay zone 1	Pay zone 2
k_h	Horizontal permeability	md	40	20
k_v	Vertical permeability	md	4	2
B_o	Oil formation volume factor	res bbl/STB	1.1	1.1
μ	Viscosity of oil	cp	1	1
r_e	Drainage radius	ft	1489	1489
r_w	Wellbore radius	ft	0.328	0.328
s	Skin	Dimensionless	16	10
P_R	Reservoir pressure	psi	3500	3200
P_{wf}	Bottomhole flowing pressure	psi	2000	1635
T_R	Reservoir temperature	°F	200	200
h	Height	ft	100	60

a	Width of reservoir	ft	1000	1000
b	Length of reservoir	ft	3500	3500
L	Length of lateral	ft	2500	2500

Assumptions made on the PVT data for simulation purposes. The assumption is based on a typical reservoir property of an oil well:

Table 3.2: PVT data for dual-lateral well

Description	Units	Pay zone 1	Pay zone 2
Oil gravity	°API	35	35
Gas gravity	Sp. gravity	0.7	0.7
Water salinity	ppm	80000	80000
Water cut	fraction	0	0
Gas Oil Ratio (GOR)	scf/STB	500	500

b) Model assumptions

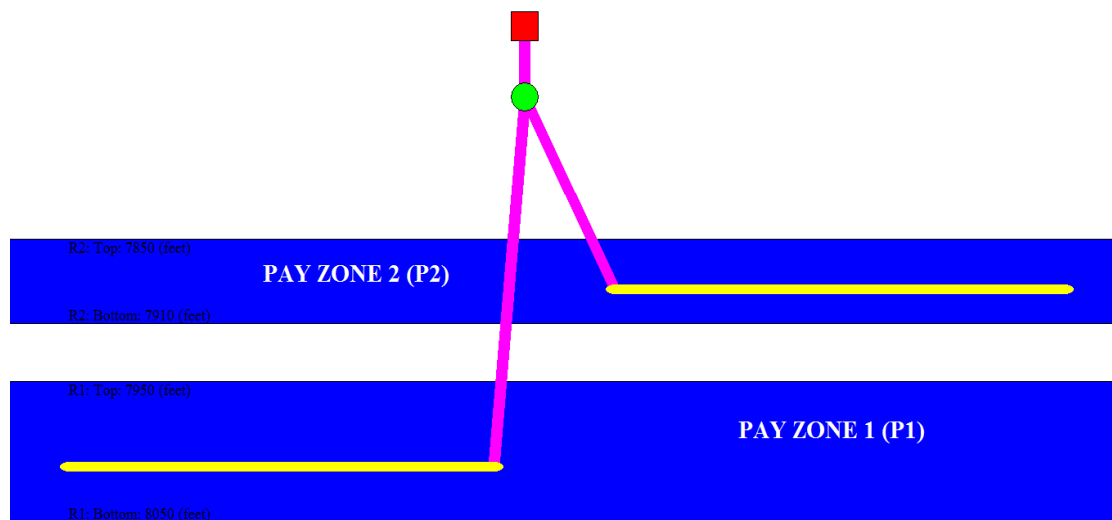


Figure 3.1: A schematic diagram of a dual-opposed lateral well

- Each lateral produces from different reservoir and the reservoir compartments are isolated from each other.
- The laterals are assumed to be horizontal such that gravity effect is neglected.
- Inflow effect on wellbore pressure drop is comparatively small and negligible.

3.1.2 Pseudo-steady state condition

a) Data availability

Reservoir and well data from Table 3.1 and Table 3.2 is applied to analyse the inflow performance of a dual-lateral well under pseudo-steady state condition.

b) Model assumptions

The well configurations are similar to Figure 3.1. The model assumptions for pseudo-steady state condition are:

- Each lateral produces from different reservoir and the reservoir are communicating with each other.
- The laterals are assumed to be horizontal such that gravity effect is neglected.
- Inflow effect on wellbore pressure drop is significant.

3.2 TRI-LATERAL WELL

3.2.1 Steady-state condition

a) Data availability

Table 3.3 presents an example of a hypothetical reservoir data for oil well taken from SPE paper by Chen *et al.*, 2000. This data was used to develop a deliverability model to predict performance of multilateral wells [17].

Table 3.3: Reservoir and well data for a tri-lateral well [17]

Symbol	Description	Units	Pay zone 1	Pay zone 2	Pay zone 3
k_h	Horizontal permeability	md	50	100	150
k_v	Vertical permeability	md	4	10	15
B_o	Oil Formation volume factor	res bbl/STB	1.1	1.1	1.1
μ	Viscosity of oil	cp	1	1	1
r_e	Drainage radius	ft	3000	3000	3000
r_w	Wellbore radius	ft	0.208	0.208	0.208
s	Skin		0	0	0
P_R	Reservoir pressure	psi	5400	5100	4900
P_{wf}	Bottomhole flowing pressure	psi	0	0	0
T_R	Reservoir temperature	°F	250	250	250
h	Height	ft	200	75	50
a	Width of reservoir	ft	1000	1000	1000
b	Length of reservoir	ft	3500	3500	3500
L	Length of lateral	ft	2000	1500	1000

Assumptions made on the PVT data for simulation purposes. The assumption is based on a typical reservoir property of an oil well:

Table 3.4: PVT data for tri-lateral well

Description	Units	Pay zone 1	Pay zone 2	Pay zone 3
Oil gravity	°API	35	35	35
Gas gravity	Sp. gravity	0.7	0.7	0.7
Water salinity	ppm	80000	80000	80000
Water cut	fraction	0	0	0
Gas Oil Ratio (GOR)	scf/STB	500	500	500

b) Model assumptions

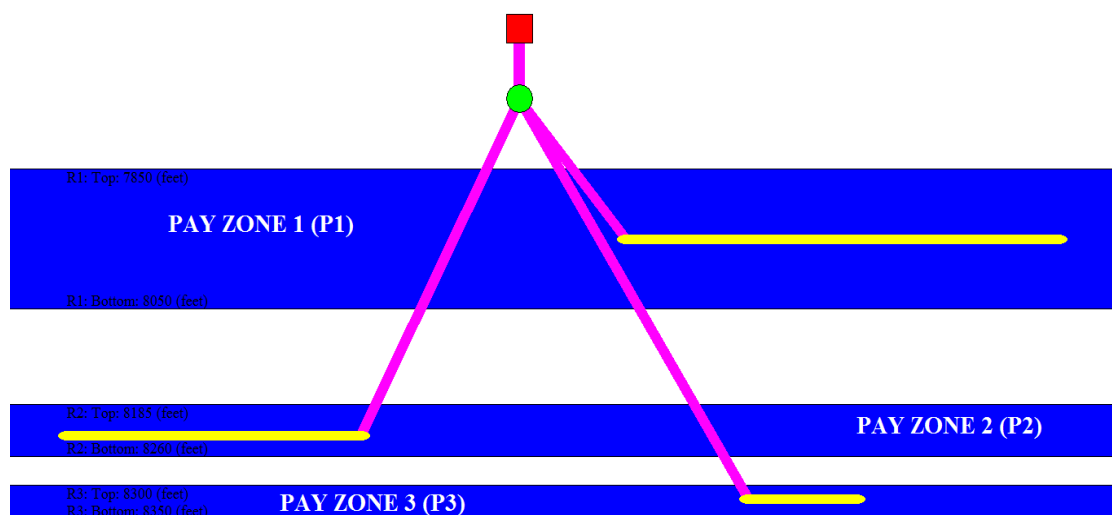


Figure 3.2: A schematic diagram of a tri-lateral well

- Each lateral produces from different reservoir and the reservoir compartments are isolated from each other.
- The laterals are assumed to be horizontal such that gravity effect is neglected.
- Inflow effect on wellbore pressure drop is comparatively small and negligible.

3.2.2 Pseudo-steady state condition

a) Data availability

Reservoir and well data from Table 3.3 and table 3.4 is applied to analyse the inflow performance of a tri-lateral well under pseudo-steady state condition.

b) Model assumptions

The well configurations are similar to Figure 3.2. The model assumptions for pseudo-steady state condition are:

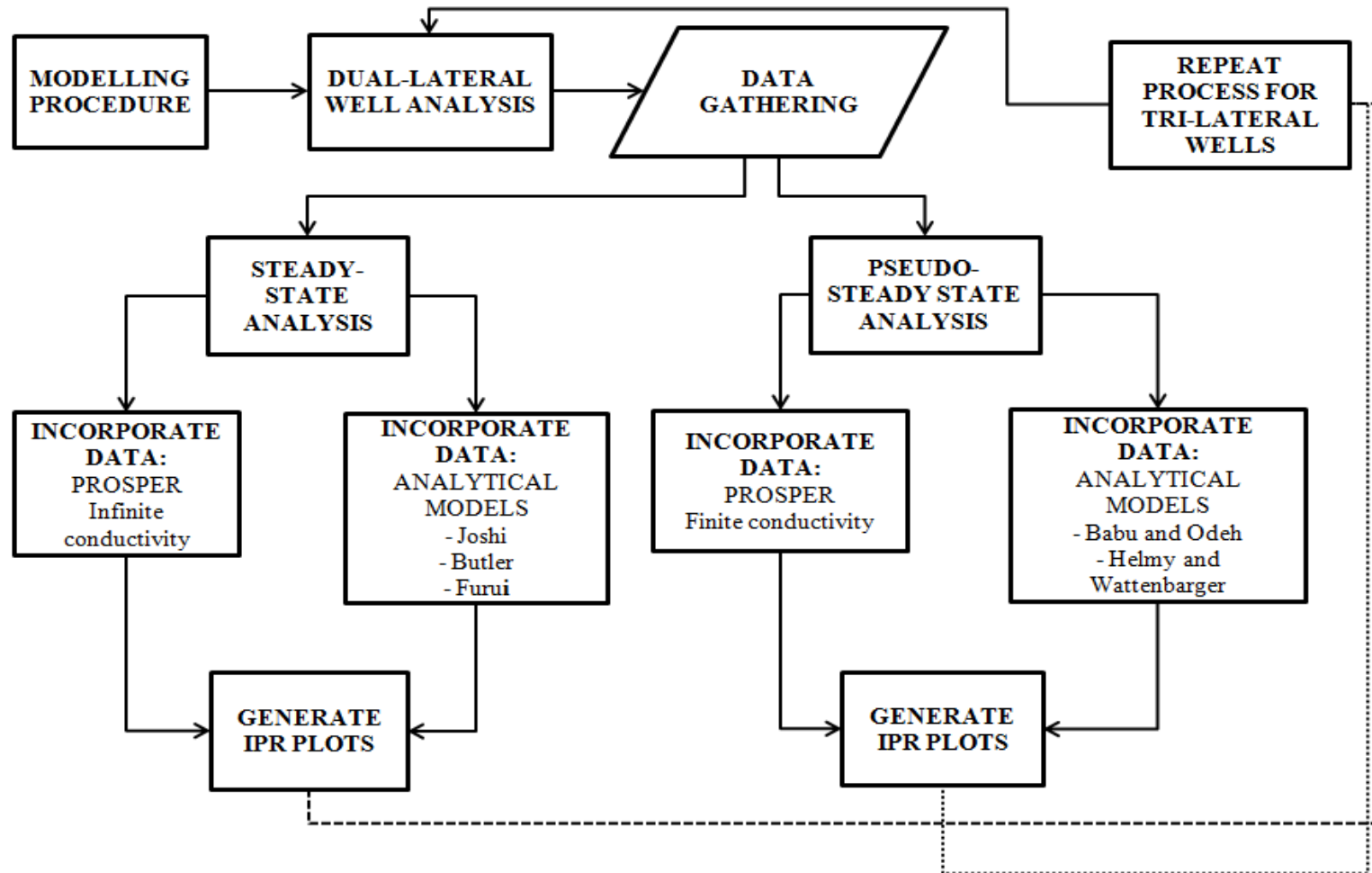
- Each lateral produces from different reservoir and the reservoir are communicating with each other.
- The laterals are assumed to be horizontal such that gravity effect is neglected.
- Inflow effect on wellbore pressure drop is significant.

3.3 MODELLING PROCEDURES

The modelling procedure is summarized in Figure 3.3.

- a) First modelling inflow performance for a dual-lateral well.
- b) Data is collected from SPE papers and dissertations related to multilateral well performance.
- c) Analysis of dual-lateral well under steady-state condition.
- d) Incorporate the available data into software (PROSPER) and analytical models.
- e) Generate Inflow Performance Relationship (IPR) models under two different conditions.
- f) Pseudo-steady state condition Comparison and matching process of IPR plots between numerical and analytical approach.
- g) The purpose of step f) is to select an analytical model to perform sensitivity study to the length of laterals.
- h) Repeat b), c), d), e) and f) for a tri-lateral well.

Figure 3.3: Workflow of the modelling procedure



3.4 WORKFLOW SUMMARY

The workflow is summarized in Figure 3.4:

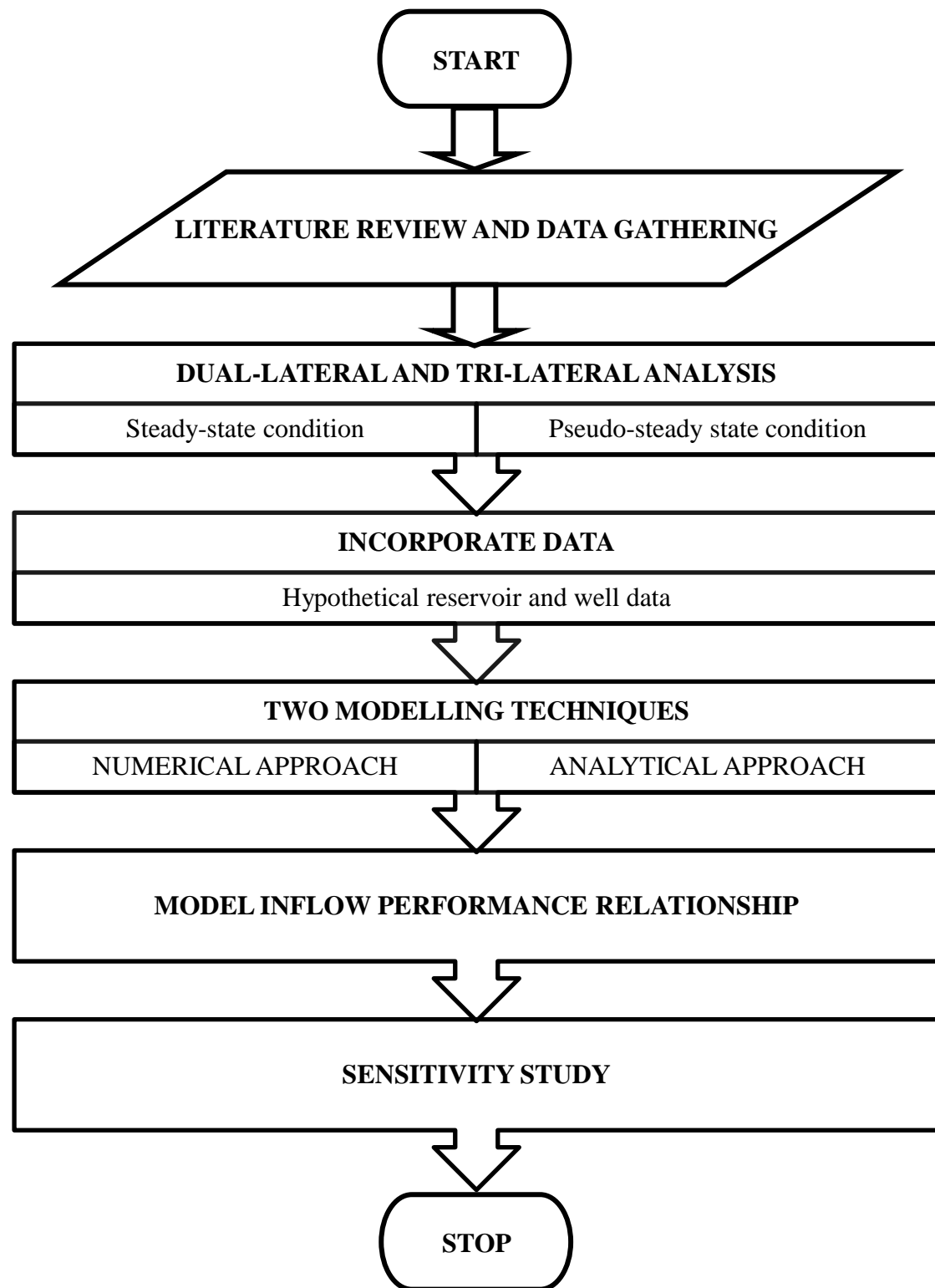


Figure 3.4: Workflow summary

CHAPTER 4

RESULTS AND DISCUSSION

The result of the analysis of inflow performance of multilateral wells are elaborated in this section:

- IPR models produced from numerical and analytical approach under steady-state condition for dual-lateral and tri-lateral well.
- IPR models produced from numerical and analytical approach under pseudo-steady state condition for dual-lateral and tri-lateral well.
- Sensitivity study of the IPR models against varying reservoir condition and well configuration.

4.1 STEADY-STATE CONDITION

4.1.1 Reservoir Inflow Performance

For dual-lateral and tri-lateral well the trend of Inflow Performance Relationship (IPR) models evaluated by numerical and analytical approach is identical. This can be observed in the following figure 4.1, 4.2, 4.3 and 4.4:

- a) Figure 4.1 shows the IPR model of a dual-lateral well evaluated by numerical approach under infinite conductivity. The plot includes the IPR for pay zone 1, pay zone 2 and the sum flowrates of the two pay zones.

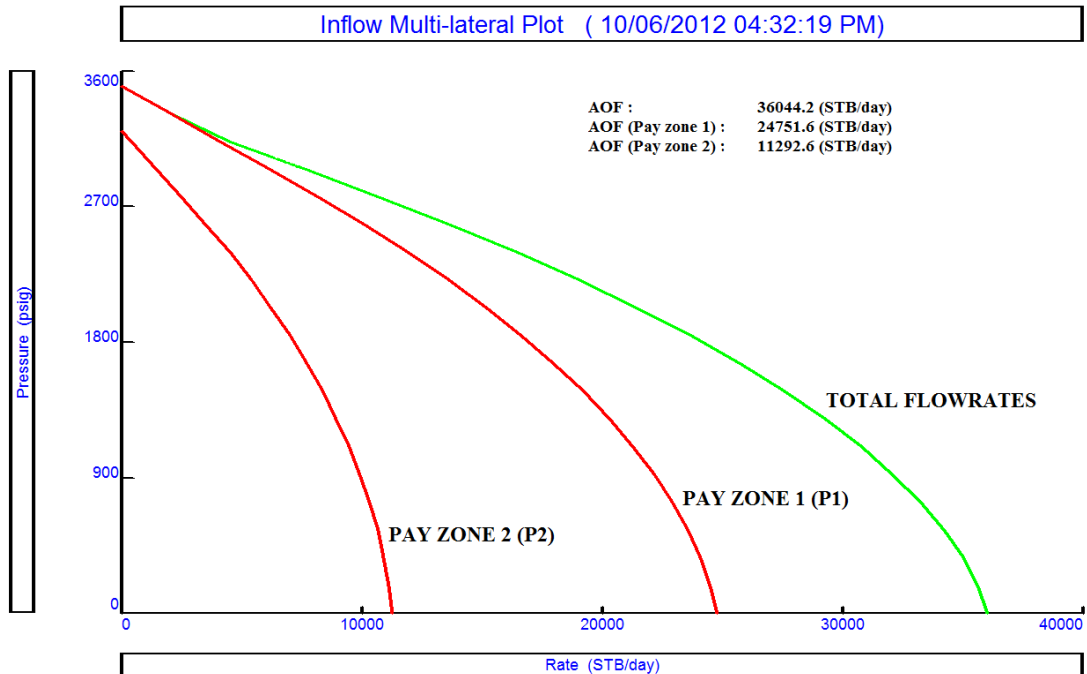


Figure 4.1: IPR from PROSPER under infinite conductivity for dual-lateral well

- b) Figure 4.2 shows the IPR model of a tri-lateral well evaluated by numerical approach under infinite conductivity. The plot includes the IPR for pay zone 1, pay zone 2, pay zone 3 and the sum flowrates of the three pay zones.

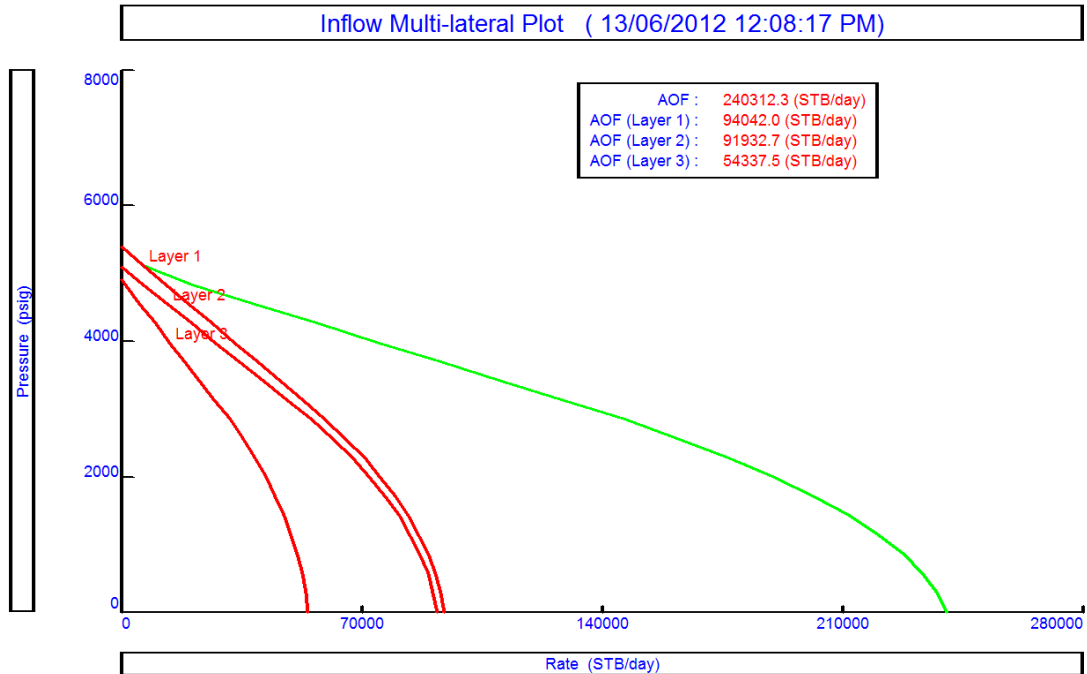


Figure 4.2: IPR from PROSPER under infinite conductivity for tri-lateral well

- c) Figure 4.3 shows the IPR model of a dual-lateral well evaluated by analytical approach under steady-state condition. The plot includes the IPR for pay zone 1, pay zone 2 and the sum flowrates of the two pay zones.

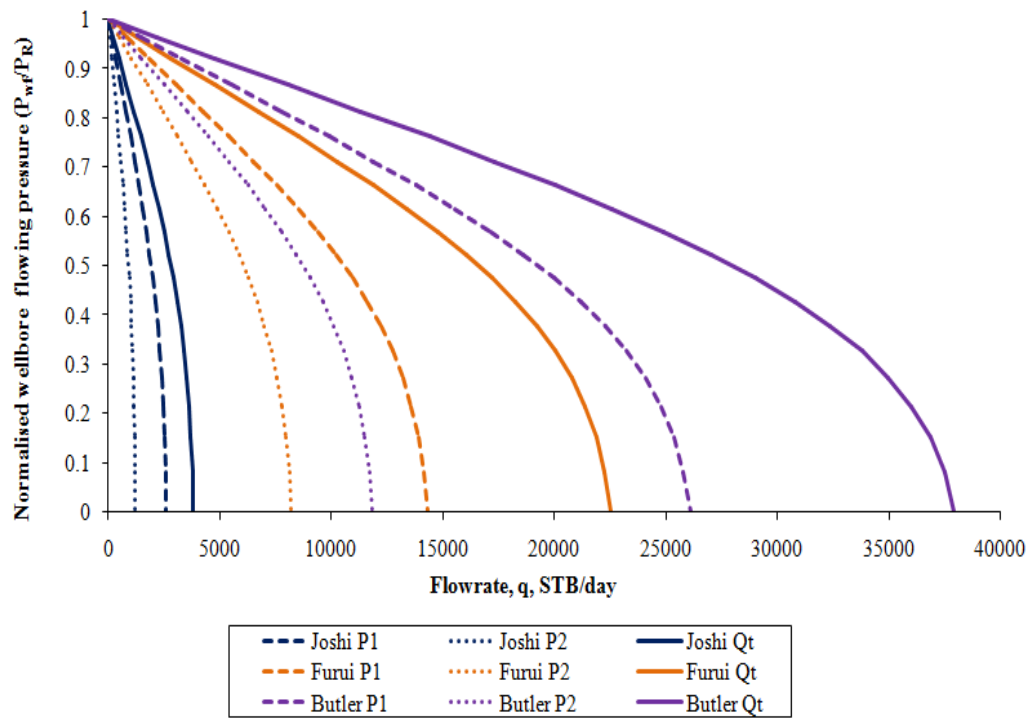


Figure 4.3: IPR of the steady-state analytical models for dual-lateral well

- d) Figure 4.4 shows the IPR model of a tri-lateral well evaluated by analytical approach under steady-state condition. The plot includes the IPR for pay zone 1, pay zone 2, pay zone 3 and the sum flowrates of the three pay zones.

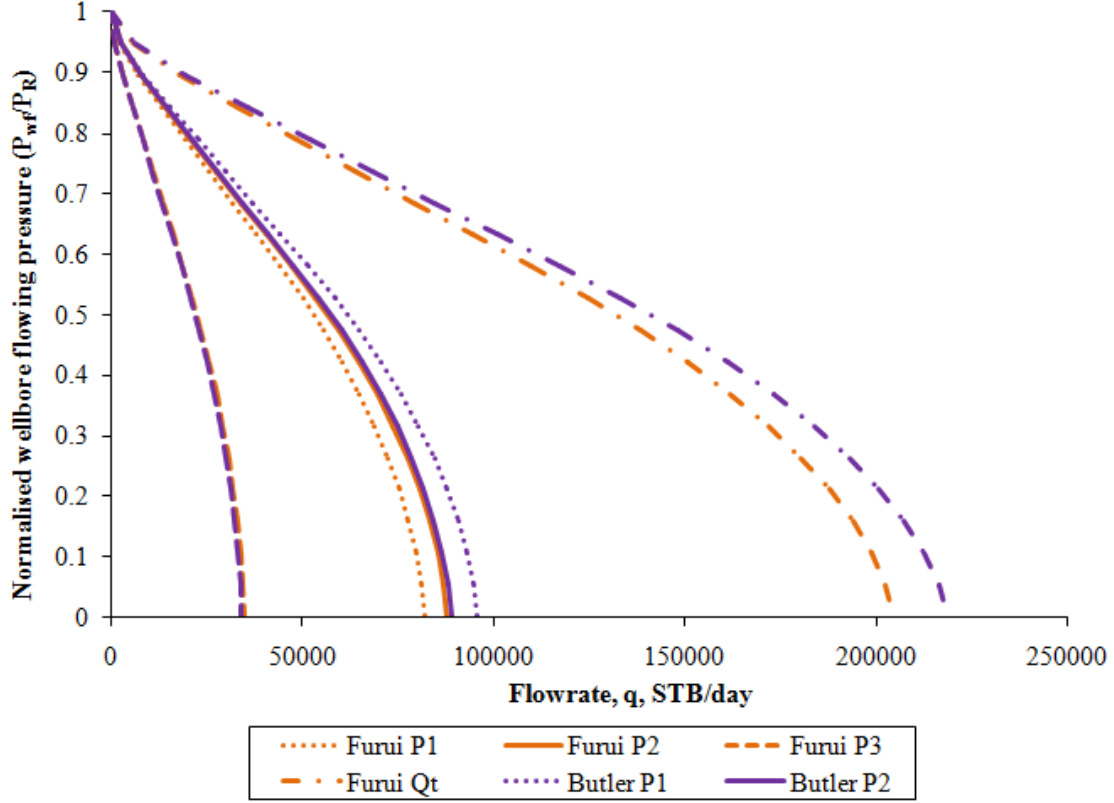


Figure 4.4: IPR steady-state analytical models for tri-lateral well

As mentioned earlier, the reservoir data used to calculate the IPR model in this project is for single phase oil wells. Therefore the expected IPR model is a straight line (undersaturated oil) however all of the figures above (Figure 4.1 to Figure 4.4) show a combination of a straight line IPR and a Vogel (Curved) IPR. The reason for this case is because the wellbore pressure is below the bubble point while the reservoir pressure is above i.e. (incompressible) liquid flow is occurring in the bulk reservoir.

For Figure 4.1 and Figure 4.3, the same trend can be observed where there is a higher flowrate in pay zone 1 than pay zone 2. This is because greater pressure drawdown is found in pay zone 1 than pay zone 2. This is the same explanation for Figure 4.2 and Figure 4.4, where flowrate of pay zone 1 is the highest in comparison with pay zone 2 and pay zone 3 while pay zone 3 has the least flowrate.

Comparing the IPR of Joshi's model (1988), Butler model (1994) and Furui *et al.*, model (2003) in Figure 15, there is a large difference in flowrates between Joshi's model and the other two models. Joshi's model exhibits the lowest flowrate in comparison with Butler model and Furui *et al.*, model. This might be due to the difference in model assumptions which lead to different IPR models. Joshi's model (1988) assumed an ellipsoidal-shaped reservoir and different assumption is made on the flow geometry. Joshi's model divided a three-flow dimensional problem into two-dimensional problems to obtain the productivity equation. Stated in SPE paper by Chen *et al.*, 2000, the solution of Joshi's model is simple and usually underestimates the productivity [17].

For Butler model (1994) and Furui *et al.*, model (2003), there is only a small difference in the flowrates relative to Joshi's model. Both models use the same system to obtain the productivity equation that is a box-shaped reservoir for a fully penetrating horizontal lateral. The two models are identical except for the constant 1.14 in the Butler model and 1.224 in the Furui *et al.*, model [13]. Furui *et al.*, model is based on Finite Element Model (FEM) simulation results while Butler is based on the law of superposition.

The same explanation for Figure 4.4 for the comparison between the steady-state analytical models however Joshi's model is not included in Figure 4.4 this might be due to the reservoir and well data used for tri-lateral well analysis that does not satisfy the condition to apply Joshi's model. The condition is:

$$L > h \text{ and } (L/2) < 0.9r_{eH}$$

4.1.2 Comparison and Matching Process

a) Dual-lateral well

Comparison of the IPR models between numerical and analytical approach is illustrated in Figure 4.5. The purpose of this process is to select an analytical model that would give the least percentage of difference with the IPR from PROSPER. Absolute Open Flow (AOF) is a useful parameter when comparing wells within a field. Therefore the AOF of each models are used to investigate which steady-state analytical models gives the least percentage of difference with PROSPER's AOF. Table 4.2 summarizes the Absolute Open Flow (AOF) of PROSPER and the analytical models.

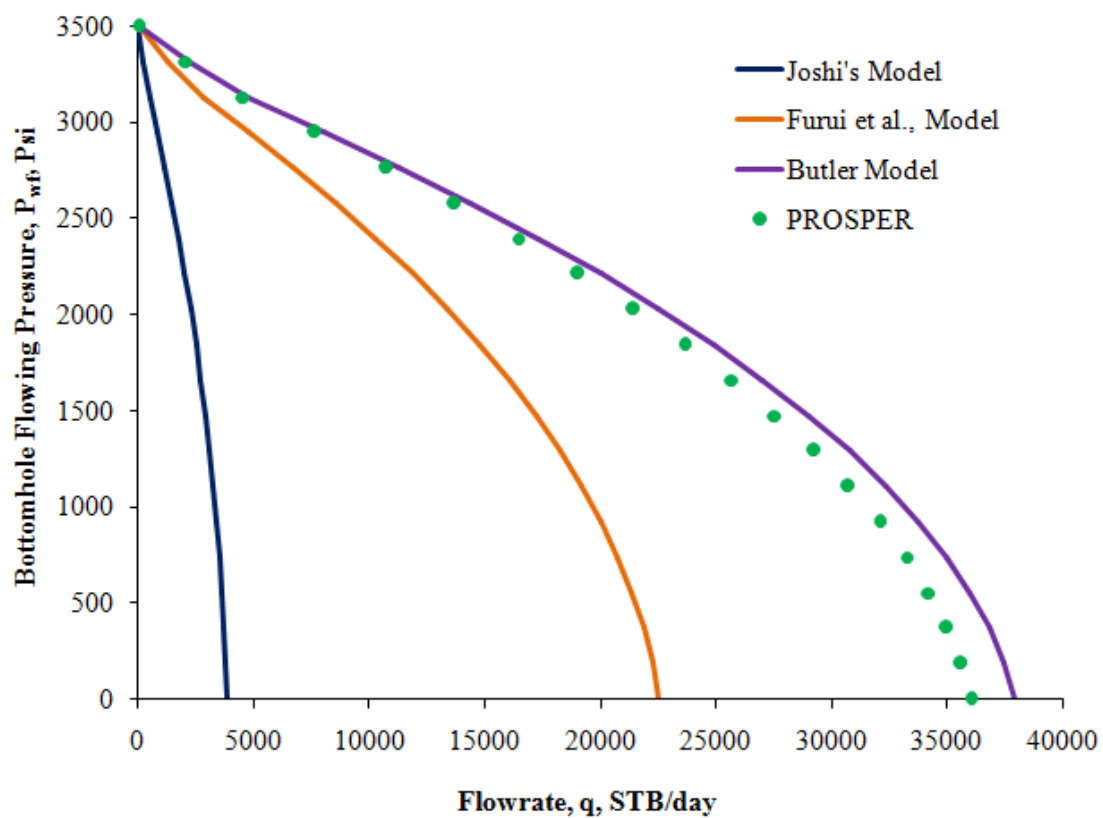


Figure 4.5: IPR of PROSPER and steady-state analytical models for dual-lateral well

Table 4.1: Comparison of the AOF of PROSPER and steady-state analytical models

	Absolute Open Flow (AOF) , STB/day		
	Pay zone 1	Pay zone 2	Total flowrates
Joshi's model (1988)	2594	1214	3808
Furui <i>et al.</i>, model (2003)	14308	8195	22504
Butler model (1994)	26087	11833	37920
PROSPER model	24751	11292	36044

Table 4.2 shows the calculated percentage of difference between the AOF of PROSPER with the AOF of the steady-state analytical models.

Table 4.2: Comparison of the percentage difference between the IPR of PROSPER and steady-state analytical models for dual-lateral well

	Percentage difference (%)		
	Pay zone 1	Pay zone 2	Total flowrates
PROSPER with Joshi's model	89.5	89.2	89.4
PROSPER with Furui <i>et al.</i>, model	42.2	27.4	37.6
PROSPER with Butler model	-5.4	-4.8	-5.2

From the results shown in Table 4.2, Butler model (1994) gives the least percentage of difference with PROSPER model hence Butler model is selected to perform sensitivity study on the well configuration. PROSPER system may be similar to the system assumed by Butler model hence the small percentage of difference between the AOF.

b) Tri-lateral well

Comparison of the IPR models between numerical and analytical approach is illustrated in Figure 4.6. The purpose of this process is to select an analytical model that would give the least percentage of difference with the IPR from PROSPER. Absolute Open Flow (AOF) is a useful parameter when comparing wells within a field. Therefore the AOF of each models are used to investigate which steady-state analytical models gives the least percentage of difference with PROSPER's AOF. Table 4.3 summarizes the Absolute Open Flow (AOF) of PROSPER and the analytical models.

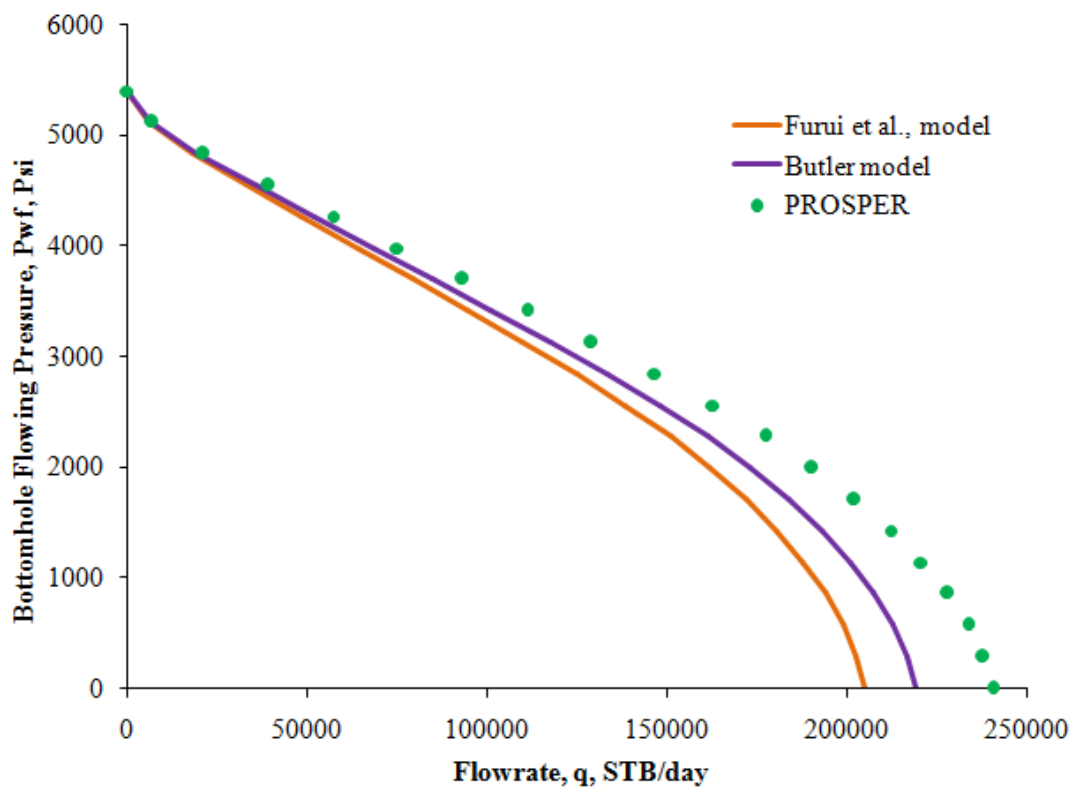


Figure 4.6: IPR of PROSPER and steady-state analytical models for tri-lateral well

Table 4.3: Comparison of the AOF of PROSPER and steady-state analytical models

	Absolute Open Flow, AOF, STB/day			
	Pay zone 1	Pay zone 2	Pay zone 3	Total flowrates
Furui <i>et al.</i>, model (2003)	82004	87737	34710	204452
Butler model (1994)	95715	88899	34070	218685
PROSPER model	94042	91932	54337	240312

Table 4.4 shows the calculated percentage of difference between the AOF of PROSPER with the AOF of the steady-state analytical models.

Table 4.4: Comparison of the percentage difference between the IPR of PROSPER and steady-state analytical models for tri-lateral well

	Percentage difference (%)			
	Pay zone 1	Pay zone 2	Pay zone 3	Total flowrates
PROSPER- Furui <i>et al.</i>, model	12.8	4.5	36.1	14.9
PROSPER - Butler model	-1.8	3.3	37.3	9

From the results shown in Table 4.4, Butler model (1994) gives the least percentage of difference with PROSPER model hence Butler model is selected to perform sensitivity study on well configuration.

4.2 PSEUDO- STEADY STATE CONDITION

4.2.1 Reservoir Inflow Performance

For dual-lateral and tri-lateral well the trend of Inflow Performance Relationship (IPR) models evaluated by numerical and analytical approach is identical. This can be observed in the following figures 4.7, 4.8, 4.9 and 4.10:

- a) Figure 4.7 shows the IPR model of dual-lateral well evaluated by numerical approach under finite conductivity. The plot includes the IPR for pay zone 1, pay zone 2 and the sum flowrates of the two pay zones.

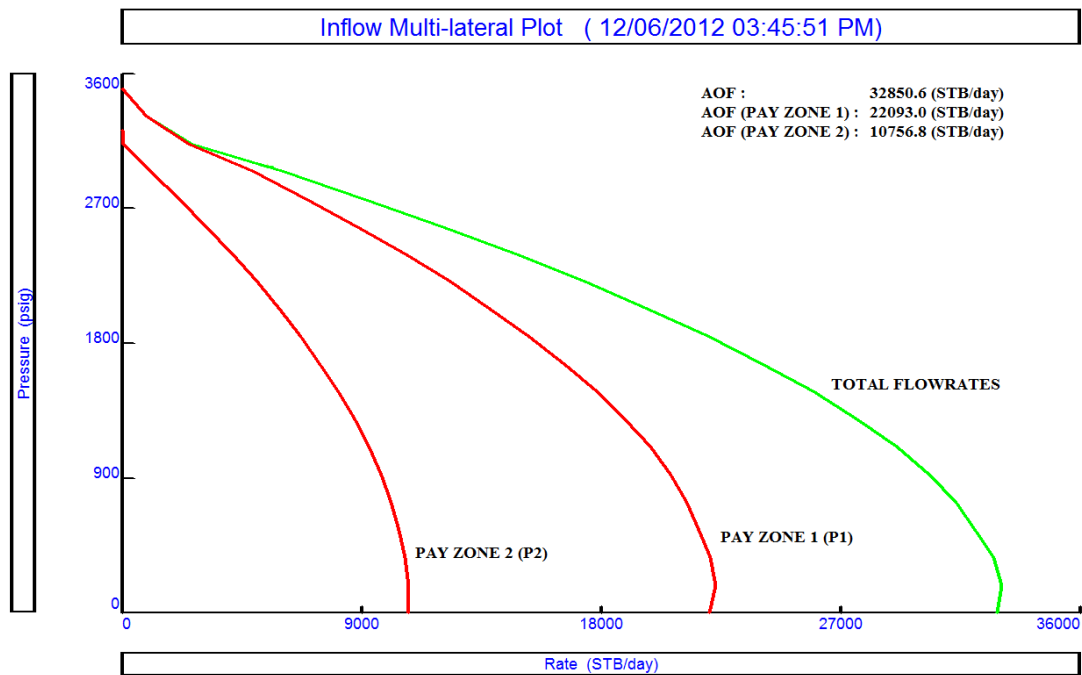


Figure 4.7: IPR from PROSPER under finite conductivity for dual-lateral well

- b) Figure 4.8 shows the IPR model of tri-lateral well evaluated by numerical approach under finite conductivity. The plot includes the IPR for pay zone 1, pay zone 2, pay zone 3 and the sum flowrates of the three pay zones.

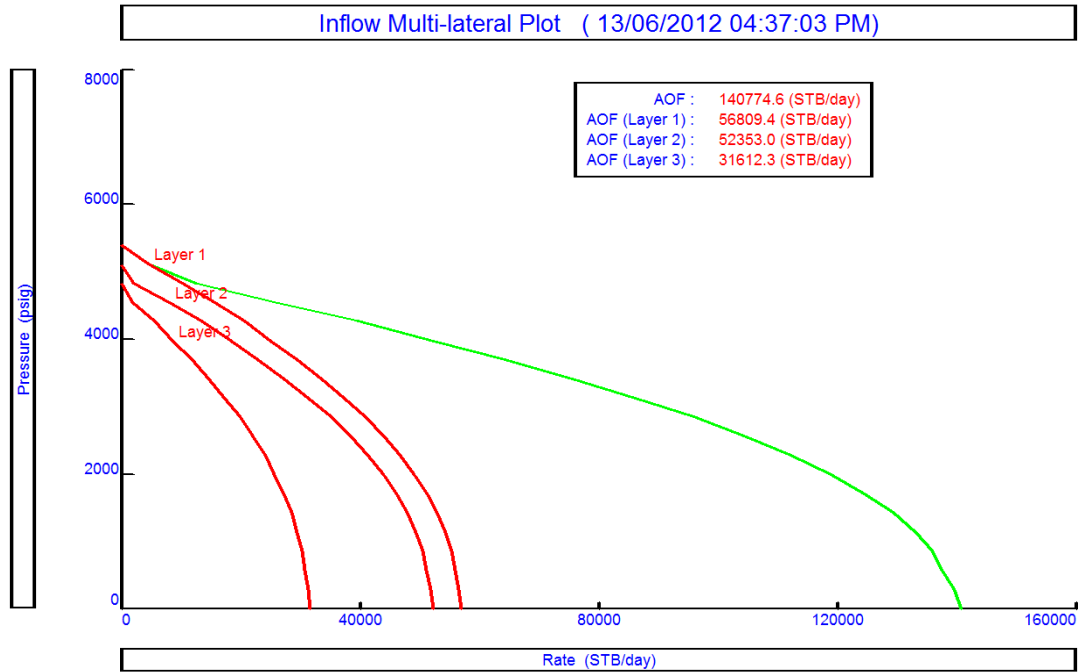


Figure 4.8: IPR from PROSPER under finite conductivity for tri-lateral well

- c) Figure 4.9 shows the IPR model of dual-lateral well evaluated by analytical approach under pseudo-steady state condition. The plot includes the IPR for pay zone, pay zone 2 and the sum flowrates of the two pay zones.

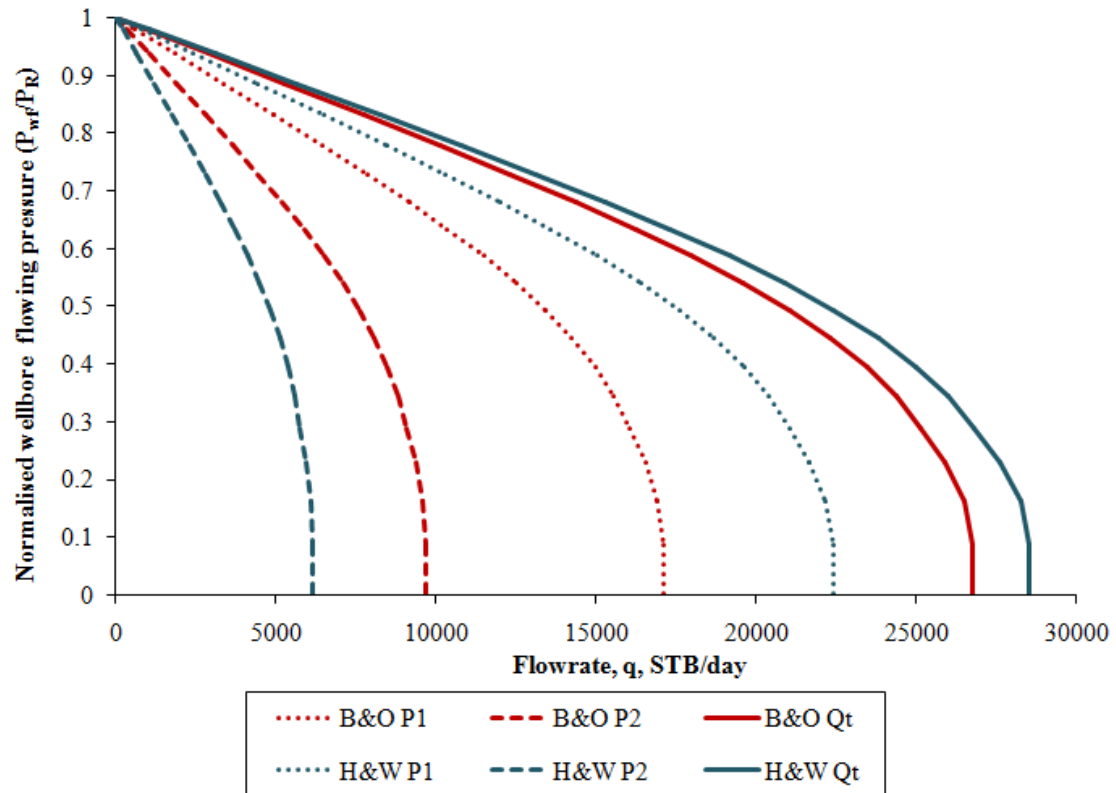


Figure 4.9: IPR of the pseudo-steady state analytical models for dual-lateral well

d) Figure 4.10 shows the IPR model of tri-lateral well evaluated by analytical approach under pseudo-steady condition. The plot includes the IPR for pay zone 1, pay zone 2, pay zone 3 and the sum flowrates of the three pay zones.

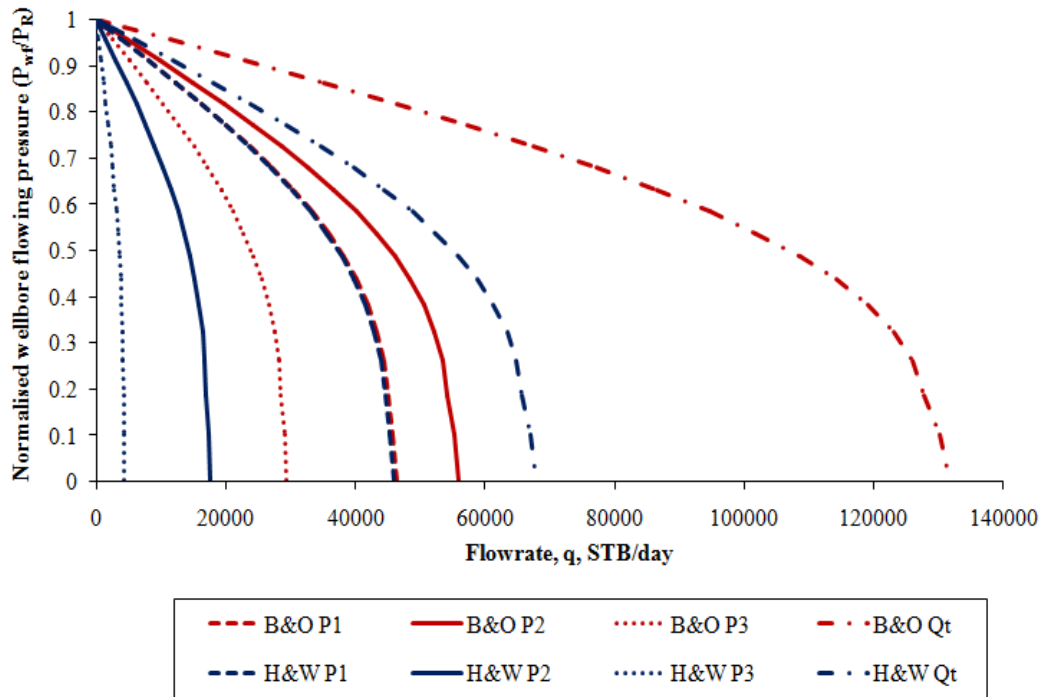


Figure 4.10: IPR of the pseudo-steady state analytical models for tri-lateral well

Again the expected IPR model is a straight line (undersaturated oil) however all of the figures above (Figure 4.7 to Figure 4.10) are showing a combination between a straight line IPR and a Vogel (Curved) IPR. The reason for this case is because the wellbore pressure is below the bubble point while the reservoir pressure is above i.e. (incompressible) liquid flow is occurring in the bulk reservoir. For Figure 4.7 and Figure 4.9, the same trend can be observed where there is a higher flowrate in pay zone 1 than pay zone 2. This is because greater pressure drawdown is found in pay zone 1 than pay zone 2. This is the same explanation For Figure 4.8 and Figure 4.9, where flowrate of pay zone 1 is the highest in comparison with pay zone 2 and pay zone 3 while pay zone 3 have the least flowrate.

Comparison of Babu & Odeh IPR model (1989) and Helmy & Wattenbarger IPR model (1998); there is only a small difference between the total flowrates. This is

because both models are almost identical. Helmy and Wattenbarger model is an extended work of Babu and Odeh model [13]. There are two parameters modified by Helmy and Wattenbarger that is the dietz shape factor and partial penetration skin factor.

4.2.2 Comparison and Matching Process

a) Dual-lateral well

Comparison of the IPR models between numerical and analytical approach is illustrated in Figure 4.11. The AOF of each models are used to investigate which pseudo-steady state analytical model gives the least percentage of difference with PROSPER's AOF. Table 4.5 summarizes the Absolute Open Flow (AOF) of PROSPER and the analytical models.

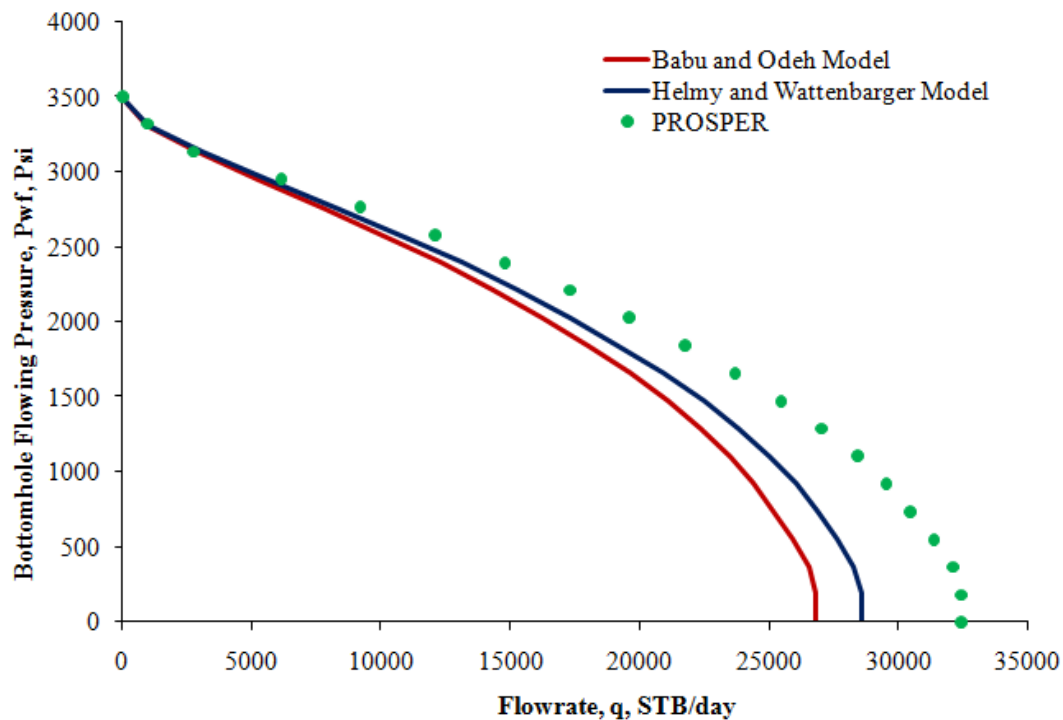


Figure 4.11: IPR of PROSPER and pseudo-steady state analytical models for dual-lateral well

Table 4.5: Comparison of the AOF of PROSPER and pseudo-steady state analytical models for dual-lateral well

	Absolute Open Flow, AOF, STB/day		
	Pay zone 1	Pay zone 2	Total flowrates
Babu & Odeh model (1989)	17090	9686	26776
Helmy & Wattenbarger model (1998)	22400	6146	28546
PROSPER model	22093	10757	32850

Table 4.6 shows the calculated percentage of difference between the AOF of PROSPER with the AOF of the pseudo-steady state analytical models.

Table 4.6: Comparison of the percentage difference between the IPR of PROSPER and pseudo-steady state analytical models for dual-lateral well

	Percentage difference (%)		
	Pay zone 1	Pay zone 2	Total flowrates
PROSPER with Babu and Odeh	21.6	8.8	17.4
PROSPER with Helmy and Wattenbarger	-2.7	42.1	12.0

The IPR of Helmy and Wattenbarger model (1998) gives the least percentage of difference with IPR of PROSPER model. Therefore this model is chosen to perform sensitivity study on well configuration.

b) Tri-lateral well

Comparison of the IPR models between numerical and analytical approach is illustrated in Figure 4.12. The AOF of each models are used to investigate which pseudo-steady state analytical model gives the least percentage of difference with PROSPER's AOF. Table 4.7 summarizes the Absolute Open Flow (AOF) of PROSPER and the analytical models.

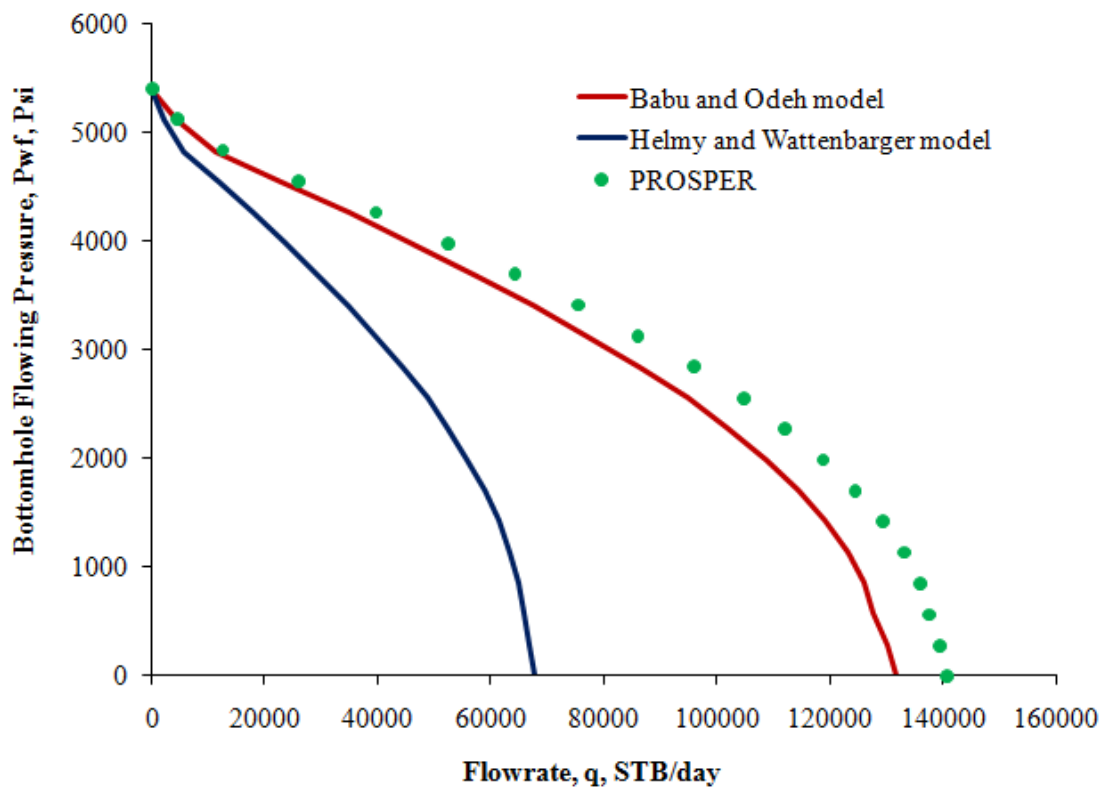


Figure 4.12: IPR of PROSPER and pseudo-steady state analytical models for tri-lateral well

Table 4.7: Comparison of the AOF of PROSPER and pseudo-steady state analytical models for tri-lateral well

	Absolute Open Flow, AOF, STB/day			
	Pay zone 1	Pay zone 2	Pay zone 3	Total flowrates
Babu & Odeh model (1989)	46411	55905	29438	131756
Helmy & Wattenbarger model (1998)	45949	17547	4330	67827
PROSPER model	56809	52353	31612.3	140774

Table 4.8 shows the calculated percentage of difference between the AOF of PROSPER with the AOF of the pseudo-steady state analytical models.

Table 4.8: Comparison of the percentage difference between the IPR of PROSPER and pseudo-steady state analytical models for tri-lateral well

	Percentage difference (%)			
	Pay zone 1	Pay zone 2	Pay zone 3	Total flowrates
PROSPER-Babu and Odeh	-6.8	6.9	6.4	-6.8
PROSPER - Helmy and Wattenbarger	19.1	66.5	86.3	51.8

Once again, the IPR of Babu and Odeh model (1989) gives the least percentage of difference with IPR of PROSPER model. Therefore Babu and Odeh model is chosen to perform sensitivity study on well configuration.

For dual-lateral and tri-lateral well under steady-state and pseudo-state condition, the AOF under steady-state condition is higher than under pseudo-steady state condition this is because multilateral interference in the reservoir for pseudo-steady state condition. The laterals are being drilled in communicating reservoirs, the drainage areas will eventually overlap. The resulting drainage area will be less than twice the drainage area for a single horizontal lateral [2].

4.3 SENSITIVITY STUDY

The results for sensitivity analysis are:

a) Well configuration: Length of laterals

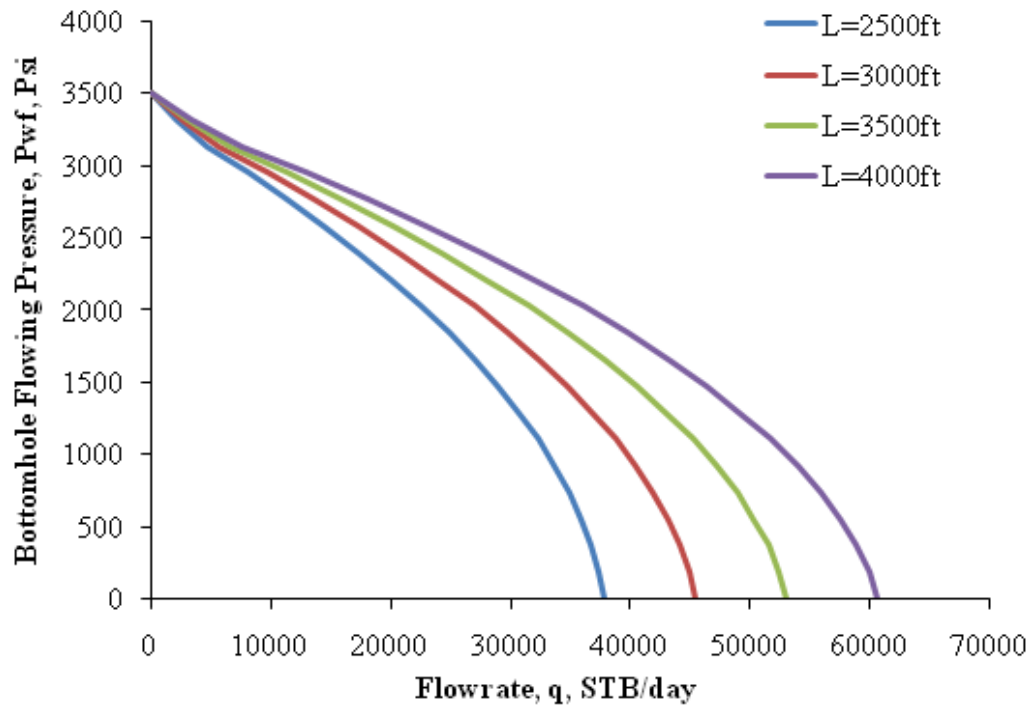


Figure 4.13: Effect of lateral lengths on the IPR under steady-state condition

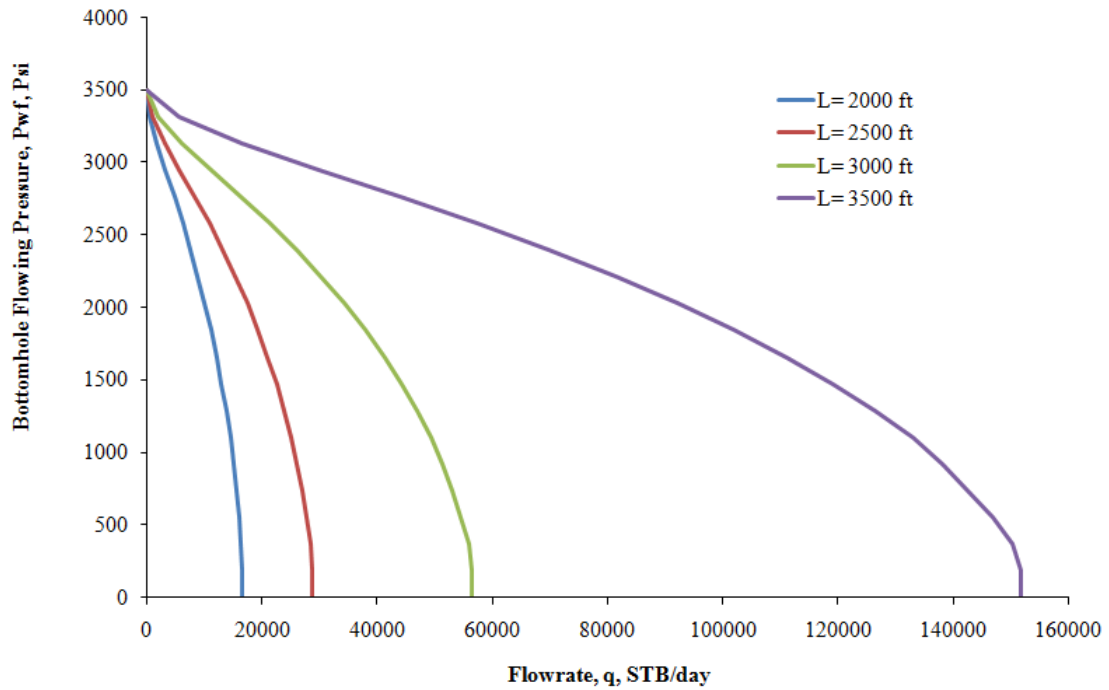


Figure 4.14: Effect of lateral lengths on the IPR under pseudo-steady condition

The trend observed in Figure 4.13 and Figure 4.14 as the well length increase the flowrate also increases this may be due to more contact area with the reservoir. However in reality, this is not true, well productivity is not proportional to the length of well as the well length increases the transportation of large volumes of fluid result in considerable pressure loss consequently decreasing well productivity.

b) Effect of Gas Oil Ratio (GOR)

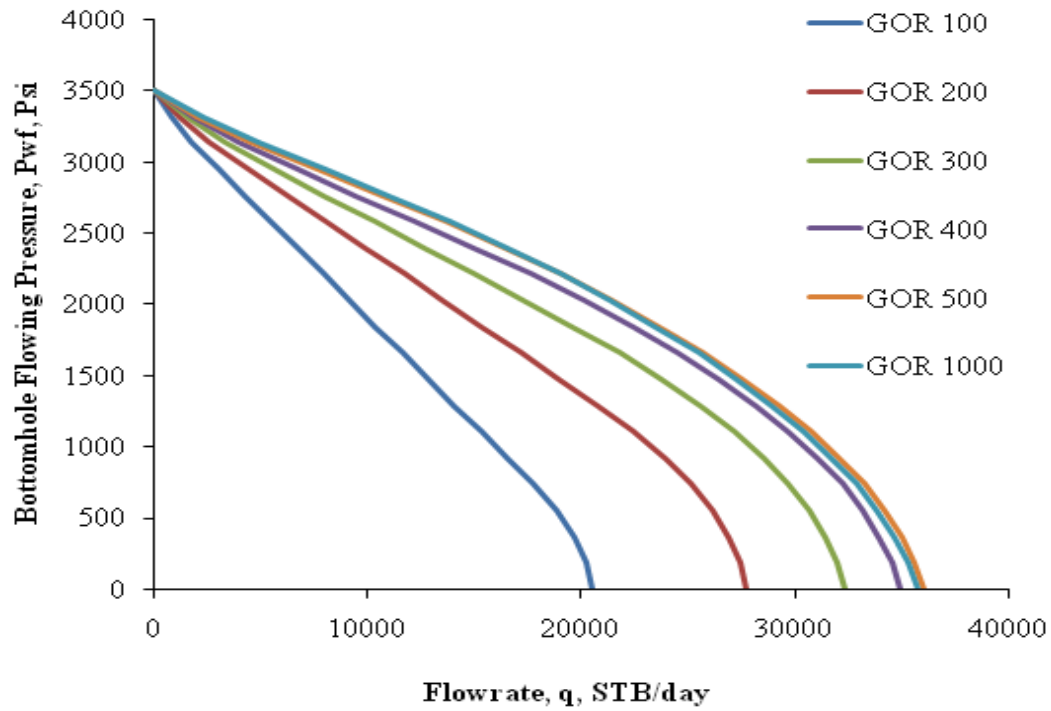


Figure 4.15: Effect of GOR on the IPR under steady-state condition

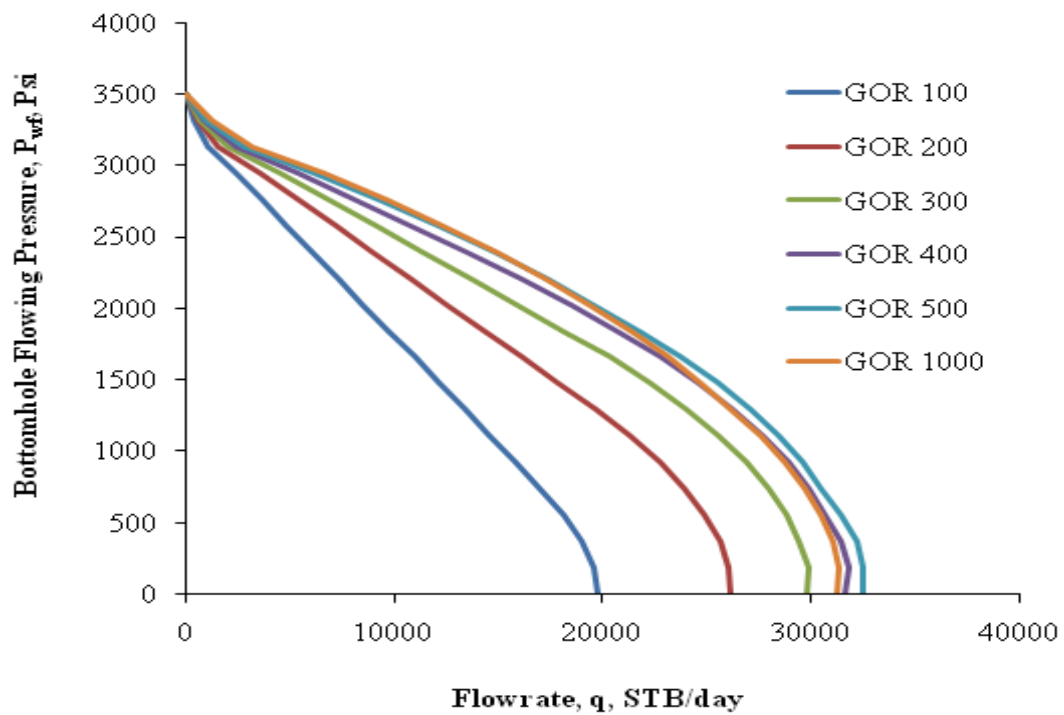


Figure 4.16: Effect of GOR on the IPR under pseudo-steady state condition

Figure 4.15 and Figure 4.16 illustrates the effect of Gas Oil Ratio (GOR) under steady-state and pseudo-steady state condition respectively for a dual-lateral well. As GOR increases from 100 scf/STB to 400 scf/STB the total production rate also increases. However from GOR 400 scf/STB onwards there is no increase in flowrate. The explanation for this is presence of gas decreases density of oil resulting in an increase in flowrate. However, there is a certain GOR known as the limiting GOR where the flowrate does not increase with an increase in GOR. High velocity of fluid in tubing causes friction and reducing the hydrostatic pressure consequently reducing production. This is one of the useful parameter to decide which artificial lift equipment is appropriate to develop the field and also when is the optimum time to install and start operating the artificial lift equipment.

c) Effect of oil gravity

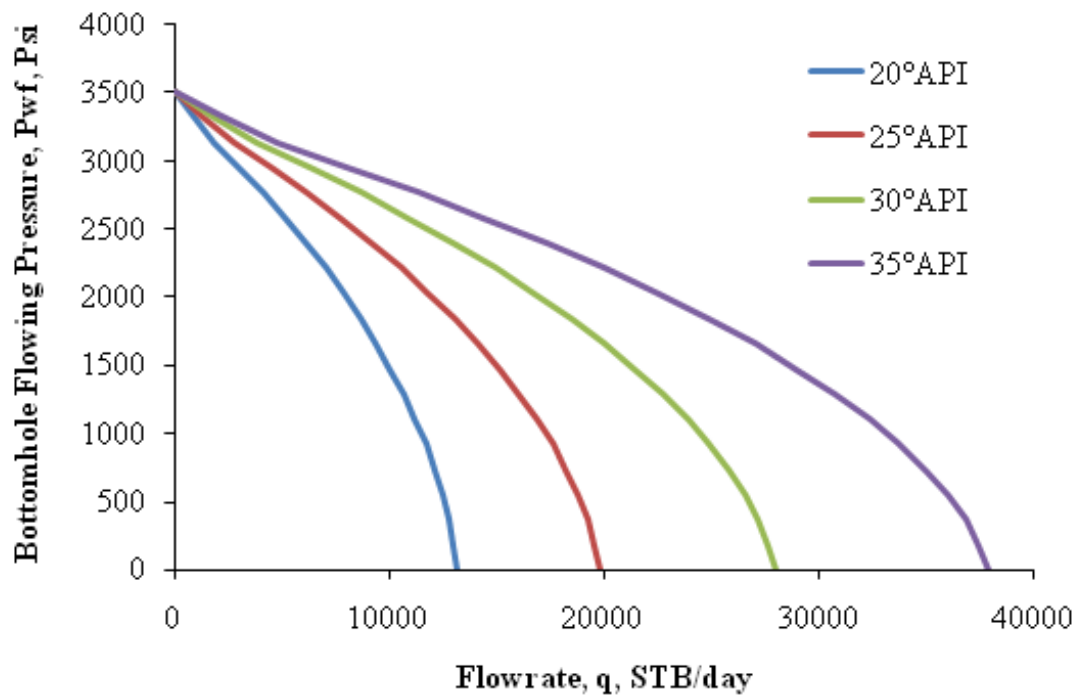


Figure 4.17: Effects of oil gravity on the IPR under steady-state condition

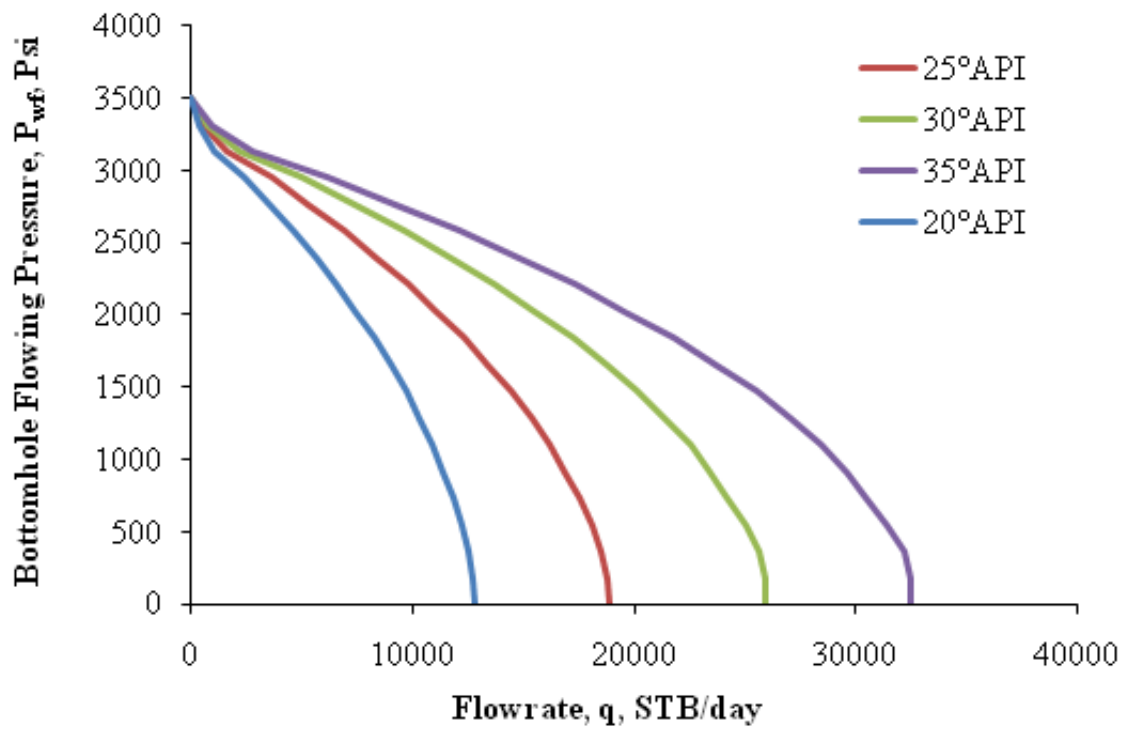


Figure 4.18: Effects of oil gravity on the IPR under pseudo-state condition

Figure 4.17 and Figure 4.18 illustrates the effect of oil gravity under steady-state and pseudo-steady state condition respectively for a dual-lateral well. At low oil gravity, the total production rate is much lower than the production rate at high oil gravity. This is because at low oil gravity, oil viscosity is high, since well productivity index is inversely proportional to the viscosity of fluid, the lower the oil gravity, the lower and the well productivity index.

CHAPTER 5

CONCLUSION AND RECOMMENDATION

The conclusion that can be drawn from the results and discussions are:

The trend of IPR models simulated from numerical and analytical approach under steady-state and pseudo-steady state condition for dual-lateral and tri-lateral well is identical. The IPR models are a combination of a straight line and Vogel IPR model. This is explained in the previous chapter. This relationship between flowrate (q) and the wellbore pressure (P_{wf}) is one of the major building blocks for a nodal-type analysis of well performance [16].

The sensitivity study shows that:

- Effects of well length: Increasing the length, the production rate also increases however this is incorrect. In reality, longer length of laterals results in a larger pressure loss hence decreasing productivity.
- Effects of GOR: Increasing GOR, the production rate also increases until a certain GOR is reached where there is no increase in production rate. This is known as the limiting GOR.
- Effects of oil gravity: At low oil gravity, the total production rate is much lower than the production rate at high oil gravity. This is because at low oil gravity, oil viscosity is high, since well productivity index is inversely proportional to the viscosity of fluid, the lower the oil gravity, the lower and the well productivity index.

Further recommendations to extend the project are:

- a) Analytical approach provides a swift determination of multilateral well deliverability. However, the sensitivity analyses on the length of laterals performed by the analytical models are incorrect hence for future work either modify the existing analytical models or develop a new mathematical model to

give a correct trend of results. Also, incorporate parameters such as well inclination and number of laterals in the models. The existing analytical models can be improved with the data obtained from PROSPER.

b) Also for future work, perform production optimisation for a multilateral well:

- Cased hole of open hole
- Artificial lift equipment
- Sand control requirement
- Tubing size optimisation

Carry out a nodal-type analysis of multilateral well performance therefore need to simulate IPR curve as well as Vertical Lift Performance (VLP) curve.

REFERENCES

- [1] A. Retnanto, "Petroleum Production Optimization Using Horizontal and Multilateral Wells," Texas A&M University, PhD Thesis 1998.
- [2] University Heriot-Watt, "Advanced Well Completion," in *Production Technology Notes*. United Kingdom, 2010, ch. Chapter 2.
- [3] Mike R. Chambers, "Multilateral technology gains broader acceptance," *Oil and gas Journal*, p. 4, 1998.
- [4] Abdel-Alim H. El-Sayed and Mohammed M. Amro, "Production Performance of Multilateral Wells," in *SPE/IADC Middle East Drilling Technology Conference*, 1999, p. 12.
- [5] A.D. Hill, D. Zhu, and M.J. Economides, "Introduction: Purposes and Applications of Multilateral Wells," in *Multilateral Wells*.: Society of Petroleum Engineers, 2008, ch. Chapter 1.
- [6] T. Yildiz, "Multilateral Horizontal Well Productivity," in *SPE Europec/EAGE Annual Conference*, 2005, p. 8.
- [7] A.D. Hill, D. Zhu, and M.J. Economides, "Application of Complex Well Architecture to Common Geological Settings," in *Multilateral Wells*.: Society of Petroleum Engineers, 2008, ch. Chapter 2.
- [8] Dulce Maria Arcos Rueda, "Technical, Economic and Risk Analysis of Multilateral Wells," Texas A&M University, MSc Thesis 2008.
- [9] Schlumberger, "Multiple Questions and Intelligent Answers," *Middle East and Asia Reservoir Review*, 2001.
- [10] M.J. Economides, L.T. Watters, and Shari Dunn-Norman, *Petroleum Well Construction*.: Wiley, John & Sons, Incorporated, 1998.
- [11] R. Kamkom, "Modeling Performance of Horizontal, Undulating and Multilateral Wells," Texas A&M University, PhD Thesis 2007.
- [12] Petroleum Experts IPM, *PROSPER User Guide*., 1990 - 2007.
- [13] A.D. Hill, D. Zhu, and M.J. Economides, "Multilateral Well Performance," in *Multilateral Wells*.: Society of Petroleum Engineers, 2008, ch. Chapter 5.
- [14] R. Kamkom and D. Zhu, "Generalized Horizontal Well Inflow Performance

Relationships for Liquid, Gas, or Two-phase Flow," in *SPE/DOE Symposium in Improved Oil Recovery*, 2006.

- [15] Heriot-Watt University, "Radial Flow," in *Well Test Analysis.*, 2010, ch. Chapter 1.
- [16] University Heriot-Watt, "Reservoir and Tubing Performance," in *Production Technology.*, 2010, ch. Chapter 3.
- [17] W. Chen, D. Zhu, and A.D. Hill, "A Comprehensive Model of Multilateral Well Deliverability," in *SPE International Oil and Gas Conference*, 2000, p. 9.
- [18] A Goffart, "La complétion et la production en drains horizontaux," in *AFTP/SPE France Conference*, 1998.
- [19] M. Tabatabaei and A. Ghalambor, "A New Method To Predict Performance of Horizontal and Multilateral Wells," *SPE Production and Operations*, pp. 75-87, 2011.

APPENDICES

Appendix A

Below is a diagram that illustrates the level of sophistication in the design of multilateral wells by Technical Advancement of Multilaterals (TAML) level.

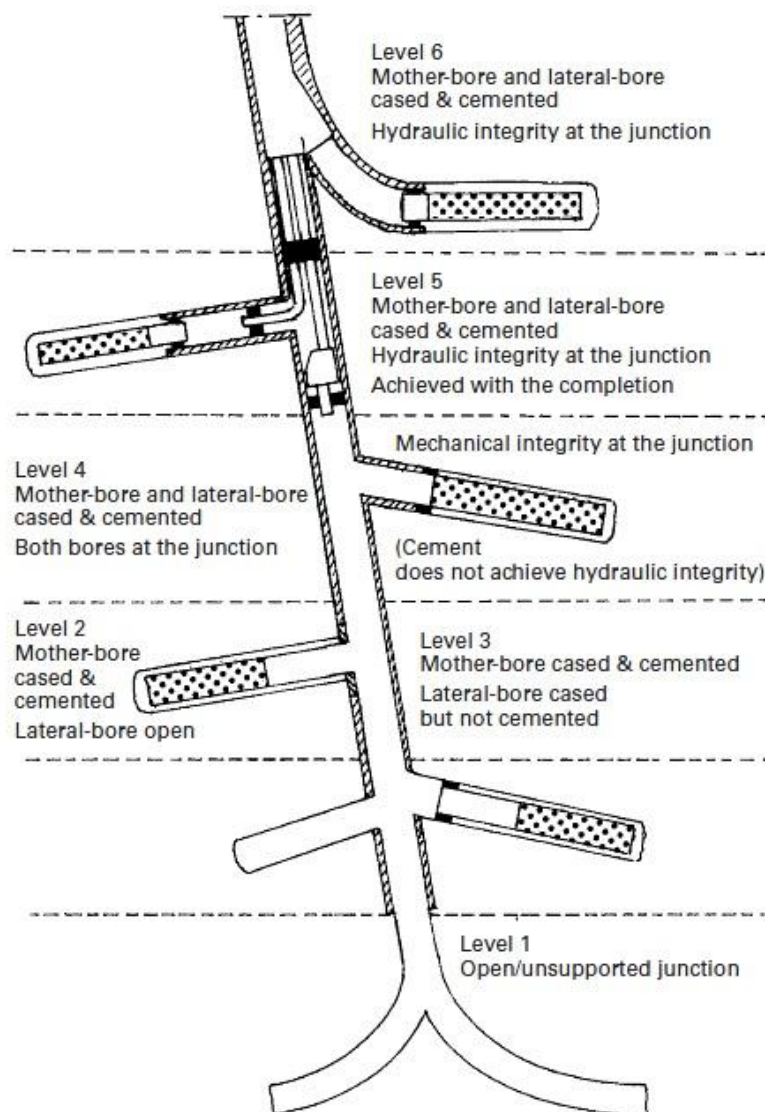


Figure A.1: TAML classification for multilateral wells [18]

Appendix B

Babu and Odeh model (1989)

The partial penetration skin, S_R , is evaluated for two different cases, depending on the horizontal dimensions of the reservoir:

Case 1: $a > b$	Case 2: $b > a$
Case 1, the reservoir extends farther in the horizontal direction perpendicular to the well than in the direction of the wellbore trajectory.	Case 2, the reservoir extends farther in the direction of the wellbore trajectory than in the horizontal direction perpendicular to the well.

The particular criteria for case 1 are:

$$\frac{a}{\sqrt{k_y}} \geq 0.75 \frac{b}{\sqrt{k_x}} > 0.75 \frac{h}{\sqrt{k_z}} \quad - \quad (B-1)$$

Then

$$S_R = P_{xyz} + P'_{xy} \quad - \quad (B-2)$$

where

$$P_{xyz} = \left(\frac{b}{L} - 1\right) \left[\ln\left(\frac{h}{r_w}\right) + 0.25 \ln \frac{k_x}{k_z} - \ln\left(\sin \frac{\pi z}{h}\right) - 1.84 \right] \quad - \quad (B-3)$$

and

$$P'_{xy} = \frac{2b^2}{Lh} \sqrt{\frac{k_z}{k_x}} \left\{ F\left(\frac{L}{2b}\right) + 0.5 \left[F\left(\frac{4x_{mid} + L}{2b}\right) - F\left(\frac{4x_{mid} - L}{2b}\right) \right] \right\} \quad - \quad (B-4)$$

Where x_{mid} is the x-coordinate of the midpoint of the well,

$$x_{mid} = \frac{x_1 + x_2}{2} \quad - \quad (B-5)$$

and

$$F\left(\frac{L}{2b}\right) = -\left(\frac{L}{2b}\right) \left[0.145 + \ln\left(\frac{L}{2b}\right) - 0.137\left(\frac{L}{2b}\right)^2 \right] \quad - \quad (B-6)$$

$F\left(\frac{4x_{mid}+L}{2b}\right)$ and $F\left(\frac{4x_{mid}-L}{2b}\right)$ in Equation B-4 are evaluated as following. If the values of $\left(\frac{4x_{mid}+L}{2b}\right)$ and $\left(\frac{4x_{mid}-L}{2b}\right)$ are less than or equal to 1, $F\left(\frac{4x_{mid}+L}{2b}\right)$ and $F\left(\frac{4x_{mid}-L}{2b}\right)$ are calculated using the following equation with the argument $L/2b$ replaced by $\left(\frac{4x_{mid}+L}{2b}\right)$ and/or $\left(\frac{4x_{mid}-L}{2b}\right)$,

$$\left(\frac{L}{2b}\right) = -\left(\frac{L}{2b}\right) \left[0.145 + \ln\left(\frac{L}{2b}\right) - 0.137\left(\frac{L}{2b}\right)^2 \right] \quad - \quad (B-7)$$

Otherwise if $\left(\frac{4x_{mid}+L}{2b}\right)$ and $\left(\frac{4x_{mid}-L}{2b}\right)$ are greater than 1, then $F\left(\frac{4x_{mid}+L}{2b}\right)$ and $F\left(\frac{4x_{mid}-L}{2b}\right)$ are calculated by,

$$F(x) = (2 - x)[0.145 + \ln(2 - x) - 0.137(2 - x)^2] \quad - \quad (B-8)$$

Where x is either $\left(\frac{4x_{mid}+L}{2b}\right)$ or $\left(\frac{4x_{mid}-L}{2b}\right)$

The criteria for case 2 are,

$$\frac{b}{\sqrt{k_x}} \geq 0.75 \frac{a}{\sqrt{k_y}} > 0.75 \frac{h}{\sqrt{k_z}} \quad - \quad (B-9)$$

For this case,

$$S_R = P_{xyz} + P_y + P_{xy} \quad - \quad (B-10)$$

where

$$P_y = \frac{6.28b^2}{ah} \frac{\sqrt{k_x k_z}}{k_y} \left[\left(\frac{1}{3} - \frac{x_{mid}}{b} + \left(\frac{x_{mid}}{b} \right)^2 \right) + \frac{L}{24b} \left(\frac{L}{b} - 3 \right) \right] \quad - \quad (B-11)$$

and

$$P_{xy} = \left(\frac{b}{L} - 1\right) \left(\frac{6.28a}{h} \sqrt{\frac{k_z}{k_x}}\right) \left(\frac{1}{3} - \frac{y_0}{a} + \left(\frac{y_0}{a}\right)^2\right) \quad - \quad (\text{B-12})$$

Where P_{xyz} in Equation B-10 is the same as defined in Equation B-3

Appendix C

Helmy and Wattenbarger model (1998)

For the uniform flux case, the shape factor is given by

$$\begin{aligned} \ln C_A = 4.485 - & \left[4.187 - 12.56 \left(\frac{y_{weq}}{a_{eq}} \right) + 12.56 \left(\frac{y_{weq}}{a_{eq}} \right)^2 \right] \left(\frac{a_{eq}}{h_{eq}} \right) \\ & + 2.0 \ln \left(\sin \left(\frac{\pi z_{weq}}{h_{eq}} \right) \right) + \ln \left(\frac{a_{eq}}{h_{eq}} \right) \end{aligned} \quad (\text{C-1})$$

And the partial penetration skin factor, SR , is

$$S_R = \left(\left(\frac{b_{eq}}{L_{eq}} \right)^{0.858} - 1 \right) (A + B) \quad (\text{C-2})$$

Where

$$A = -0.025 + 0.022 \ln C_A - 3.781 \ln \left(\frac{h_{eq}}{a_{eq}} \right) \quad (\text{C-3})$$

and

$$B = \frac{1.289 - 4.751 \left(\frac{x_{eq}}{b_{eq}} \right) + 4.652 \left(\frac{x_{eq}}{b_{eq}} \right)^2 + 1.654 \left(\frac{L_{eq}}{b_{eq}} \right) - 1.718 \left(\frac{L_{eq}}{b_{eq}} \right)^2}{\left(\frac{h_{eq}}{a_{eq}} \right) \left(\frac{a_{eq}}{b_{eq}} \right)^{1.472}} \quad (\text{C-4})$$

For the uniform wellbore pressure case, the shape factor is given by

$$\begin{aligned} \ln C_A = 2.607 - & \left[4.74 - 10.353 \left(\frac{y_{weq}}{a_{eq}} \right)^{1.115} \right. \\ & \left. + 9.165 \left(\frac{y_{weq}}{a_{eq}} \right)^{2.838} \right] \left(\frac{a_{eq}}{h_{eq}} \right)^{1.011} + 1.81 \ln \left(\sin \left(\frac{\pi z_{weq}}{h_{eq}} \right) \right) \\ & + 2.056 \ln \left(\frac{a_{eq}}{h_{eq}} \right) \end{aligned} \quad (C-5)$$

And the partial penetration skin factor, S_R , is

$$S_R = \left(\left(\frac{b_{eq}}{L_{eq}} \right)^{1.233} - 1 \right) (A + B) \quad (C-6)$$

Where

$$A = 2.894 + 0.003 \ln C_A - 0.453 \ln \left(\frac{h_{eq}}{a_{eq}} \right) \quad (C-7)$$

and

$$B = \frac{0.388 - 1.278 \left(\frac{x_{eq}}{b_{eq}} \right) + 0.715 \left(\frac{x_{eq}}{b_{eq}} \right)^2 + 1.278 \left(\frac{L_{eq}}{b_{eq}} \right) - 1.215 \left(\frac{L_{eq}}{b_{eq}} \right)^2}{\left(\frac{h_{eq}}{a_{eq}} \right) \left(\frac{a_{eq}}{b_{eq}} \right)^{1.711}} \quad (C-8)$$

$$k_{eq} = \sqrt[3]{k_x k_y k_z} \quad (C-9)$$

$$x_{eq} = \sqrt{\frac{k_{eq}}{k_x}} x \quad (C-10)$$

$$y_{eq} = \sqrt{\frac{k_{eq}}{k_y}} y \quad (C-11)$$

$$z_{eq} = \sqrt{\frac{k_{eq}}{k_z}} z \quad (C-12)$$

$$x_{weq} = \sqrt{\frac{k_{eq}}{k_x}} x_w \quad (C-13)$$

$$y_{weq} = \sqrt{\frac{k_{eq}}{k_y}} y_w \quad (C-14)$$

$$z_{weq} = \sqrt{\frac{k_{eq}}{k_z}} z_w \quad (C-15)$$

$$a_{eq} = \sqrt{\frac{k_{eq}}{k_x}} a \quad (C-16)$$

$$b_{eq} = \sqrt{\frac{k_{eq}}{k_y}} b \quad (C-17)$$

$$h_{eq} = \sqrt{\frac{k_{eq}}{k_z}} h \quad (C-18)$$

$$L_{eq} = \sqrt{\frac{k_{eq}}{k_y}} L \quad (C-19)$$

$$r_{weq} = \frac{1}{2} r_w \left(\sqrt[4]{\frac{k_x}{k_z}} + \sqrt[4]{\frac{k_z}{k_x}} \right) \quad (C-20)$$

$$A_{eq} = a_{eq} h_{eq} \quad (C-21)$$